

Identification of epigenetic regulators of fibrotic transformation in cardiac fibroblasts through bulk and single-cell CRISPR screens

Corresponding Author: Dr David Lara-Astiaso

This file contains all reviewer reports in order by version, followed by all author rebuttals in order by version.

Version 0:

Reviewer comments:

Reviewer #1

(Remarks to the Author)

Aguado-Alvaro et al. aims to characterize the role of chromatin factors in fibroblast differentiation and implicating Tip60 as a pro-fibrotic factor by demonstrating that its inhibition can be used as a therapeutic approach for cardiac fibrosis. By developing a platform to functionally study fibrotic regulators, following up with Perturb-seq, and performing functional assays, the authors uncover numerous epigenetic regulators involved in fibrosis. The work, in general, displays how high throughput approaches in combination with rigorous functional assessment can identify and confirm chromatin factors and pathways involved in cardiac fibrosis providing potential therapeutic targets. However, there is a lack of validation regarding guide and Kat5 inhibitor efficiency and some of the data is not super convincing or has a small effect. Additionally, more mechanistic work could be done to display how human cardiac fibroblasts compare to the findings identified in this paper. Overall, the manuscript needs significant revision to be acceptable for publication.

Major points

1. While the authors cite that PDGFR α can be used to distinguish resting vs. fibrotic populations in humans and mice (line 119), it would be good to demonstrate this using human cardiac fibroblasts to make this finding more relevant to disease.
2. In Fig 1f, the authors use CRISPR to ablate TGFBR1 and SMAD3, but there is no clear validation that these guides produce a knockout using sequencing, PCR, or, ideally, western blot. Additionally, there is no clear validation of the guides used in Fig 2e or Fig 7g either. Extended Data Fig 5 may be showing this information at the RNA level, but if so, it is not clarified in the text or methods and Kat5, among others, is not convincing.
3. In Fig 2c, it is not clear how a "fibrotic score" is generated. Fig 2a shows that NGS sequencing was performed to determine guide abundance in the two populations. Is this population enrichment termed "fibrotic score"? Additionally, "proliferation score" is not explained in the text and is not very relevant to the findings of the paper so should be omitted or moved to supplement.
4. Functional validation assays are very convincing. It would be nice to see the images for the collagen secretion assay, if available. Additionally, more rationale could be provided for why these specific assays were chosen.
5. Better peaks could be used for Fig 6a. In particular, Myl9 and Meox1 are not super convincing. This data would be better if quantified.
6. Kat5 chemical inhibitor was not validated by looking at RT-qPCR for changes in Kat5 gene expression. This should be added to Fig 7b as validation.
7. Fig 7d is not convincing given the scale of the differential binding score. It would also be beneficial to see accessibility in iKat5 + TGFB and Mock + TGFB treated cells via browser tracks for Tead 1-4.
8. Overall, Fig 7a-e would benefit from an unstimulated control so the readers can see how iKat5 treated cells and control cells compare.
9. Fig 7f-h is very promising. It would improve the impact of the paper to expand this data to a full figure. Additional experiments could be done including the three assays done in Fig 5 as well as ATAC-seq on the unstimulated, TGFB, and iKat5 + TGFB treated cells. Likewise, it would be highly impactful if the authors could show that isolated human cardiac fibroblasts with heart failure have a similar phenotype to the TGFB or IL1B treated cells and adding iKat5 reverses some of the cardiac fibrosis.
10. As the introduction highlights, "myocardial fibrosis is a frequent outcome of many cardiac pathologies." As such, many studies have shown fibroblast activated protein (FAP) induced by both TGFB and IL-1B treatment in vitro, which population

in the scRNA experiment is marked by FAP expression, and do any of the perturbations affect its expression?

Minor points

1. Abbreviation of chromatin factors as CF is very confusing since many people use CF as an abbreviation for cardiac fibroblasts. I would recommend changing this.
2. Serum-free expansion and selection of FACS marker data can all be in the supplement since it is methodological and not super relevant to the findings of the paper (Figure 1). It makes more sense to start the paper on the CRISPR screen.
3. Text size on Fig 3a should be increased to improve readability.
4. It is not clear how many replicates were performed for the Perturb-seq screen since the data is not displayed by replicate via UMAP.
5. Fig 5c represents 2 biological replicates with 50 technical replicates. I would like to clarify that the Kruskal-Wallis test was conducted comparing the 2 values for each condition as opposed to 100 technical replicate values because of the high level of significance.
6. Fig 5e-f can be moved to supplement.
7. Fig 7a shows the Kat5 inhibitor was applied for 7 days while the text (Line 320) says 24 hours. Please clarify.

Reviewer #2

(Remarks to the Author)

In this manuscript, the Authors aimed to identify and characterize the chromatin factors influencing fibroblast differentiation and their role in cardiac fibrosis. They conducted CRISPR screens on mouse cardiac fibroblast cells treated with TGF-B to pinpoint SRCAP, TIP60, NSL complex, HCFC1, and WDR82 as potent regulators of fibrotic states with specific readout (PDGFRa). Subsequently, the Authors investigated the effects of depleting these factors on three key processes driving fibrotic transformation: collagen deposition, stress-fiber formation, and contractility. They validated their findings using an in vitro fibrosis model. Additionally, the Authors employed ATAC-seq profiling and differential TF footprinting analysis to establish connections between these chromatin factors and the chromatin accessibility of pro-fibrotic transcription factors. Finally, they utilized a KAT5-specific chemical inhibitor (NU-9056) on murine and human cardiac fibroblasts, demonstrating its potential for therapeutic development.

The manuscript is well written and figures are well prepared.

Following are the major issues needs to be addressed to reach the conclusion of manuscript:

1. The experiments were solely conducted in vitro using fibroblast cells stimulated with TGF-B. It's essential for the Authors to verify whether the findings of the manuscript are specific to cardiac fibroblast cells or applicable to fibroblast cells from other sources – a general or specific. Experimental validation using fibroblast cells isolated from other organs is required to address this question.
2. In figures 7a-e, the Authors treated primary fibroblast cells isolated from murine cardiac tissue with a KAT5-specific chemical inhibitor followed by TGF-B treatment to demonstrate its prophylactic protective effect. To claim therapeutic relevance, experiments should be conducted in a therapeutic setup both in vitro and in vivo, utilizing a fibrotic murine model.
3. In figures 7f-h, primary fibroblast cells isolated from human cardiac tissue were treated with a KAT5-specific chemical inhibitor followed by TGF-B treatment to demonstrate its prophylactic protective effect. To establish therapeutic relevance, experiments should be conducted in a therapeutic setup, such as using fibroblasts isolated from human fibrotic heart tissue.

Minor issues:

1. Standardized nomenclature for Gene and Protein names should be rectified throughout the text. For instance, when referring to the protein KAT5, it should be capitalized consistently (line 314, 315).

Reviewer #3

(Remarks to the Author)

This article explores the role of epigenetic regulatory factors in cardiac fibroblasts during fibrogenesis. The study utilizes both bulk and single-cell CRISPR screening methods to investigate the involvement of chromatin remodelers such as Srcap and Tip60, and the NSL complex in fibrosis-related processes including collagen synthesis and cell contraction. The article proposes the inhibition of Tip60 as a reliable therapeutic approach for treating cardiac fibrosis.

Overall, this paper demonstrates the integrity of its various components. Firstly, it provides a brief introduction to the impact of cardiac fibrosis on cardiac pathology and the fibroblast-associated transformation process. Subsequently, the article provides a detailed description of the specific methods employed, including bulk and single-cell CRISPR screening and epigenetic analysis. The authors then perform epigenetic analysis using the identified regulatory factors and smoothly present the strategy of Tip60 inhibition for treating cardiac fibrosis.

The strengths of the article are notable:

1. The article employs a comprehensive research design that combines bulk and single-cell CRISPR screening, providing more comprehensive information and deeper insights. It exhibits a high level of novelty.
2. The study identifies several key regulatory factors, such as chromatin remodelers Srcap and Tip60, and the NSL complex, emphasizing their control over fibrotic states. These findings offer new perspectives and potential therapeutic targets for cardiac fibrosis.

3. The researchers demonstrate how these chromatin factors enhance the activity of fibrosis-associated transcription factors during fibroblast transformation, revealing critical nodes and mechanisms within the regulatory network.

However, there are some limitations to the study:

1. The research primarily focuses on mouse cardiac fibroblasts, with relatively limited investigation of human cardiac fibroblasts. Further experiments in this area would be beneficial.
2. The article lacks extensive in vivo animal experiments, with most of the content centered around ex vivo fibroblasts. Including more in vivo experiments would be valuable.

Nevertheless, even in its current form, this article remains highly valuable and relevant to a broad audience.

Version 1:

Reviewer comments:

Reviewer #1

(Remarks to the Author)

The authors have responded to many comments raised by reviewers; however, some issues still remain.

R1Q1 and R1Q6 - Statistical analyses should be performed for the new human data (flow data on PDGFRA and IF data on H2AZac), and point out when comparisons are not significant.

R1Q8 - Second half of the response does not adequately address original concern. It would be helpful to include unstimulated control to Extended Data Fig. 8k because it would show if the reversion goes back down to baseline.

R1Q10 – It is disappointing that FAP could not be observed in the scRNA-seq after TGFb and IL-1B treatment. This finding raises issues as to whether TGFb and IL-1B treatment in vitro is actually able to activate fibroblasts, which is a key point of the authors studies.

R2Q1 - The authors mention that Kat5 inhibition has already been shown to help with fibrosis after MI with TH1834 (PMID: 36341679). The authors should show how their drug (NU-9056) compares to an already established drug, at least in their in vitro assays, to put their results in context with previously published results.

Reviewer #2

(Remarks to the Author)

I have reviewed this manuscript previously, and I am pleased to note that all the concerns I raised have been appropriately addressed by the authors. The revisions have been thoughtfully incorporated into the manuscript. I have no further concerns and fully support the acceptance of this manuscript for publication.

Reviewer #3

(Remarks to the Author)

I have no other question. Thanks.

Version 2:

Reviewer comments:

Reviewer #4

(Remarks to the Author)

In this revised manuscript from Aguado-Alvaro et. al. authors sufficiently satisfied the major comments. It is of note however the level of fibroblast activation of patient driven fibroblast could be altered compared to de novo activation of naive cardiac fibroblast in humans. As previously noted fibroblast in post-infarction state can acquire a steady state phenotype and may already have an elevated fibrotic state and thus Tgfb stimulation may not make a bigger difference. This point would be important to add to the discussion section and address that the study did not have naive human fibroblasts to assess. Nonetheless the revision is sufficient for acceptance.

Reviewer #5

(Remarks to the Author)

1. The authors should provide more information regarding the region of the “discarded” tissue. Is it atrial appendage? Were any quality control measures performed on the human fibroblasts regarding their purity and activation state?

2. Isotype matched controls should be used for flow cytometry. Not unstained cells. What were the controls for the asma intracellular staining?
3. Authors should specify which TGF β was used in the experiments. Providing catalog numbers throughout the m&m would provide transparency. Also the term unstimulated fibroblasts is a bit misleading as the culture conditions have bFGF. The culture conditions for the fibroblasts is unclear. In the text the authors mention serum free conditions, but for the human fibroblast 10% FBS is listed. The statement that the serum free conditions maintain a rested state is not thoroughly substantiated based on the data shown in extended figure 1. The data seem to suggest that the cells might be more responsive to TGF β stimulation.
4. The authors need to clarify if the data in figures represents separate isolations, replicate wells, or different passages of fibroblasts.
5. Regarding the PDGFR α expression in human fibroblasts, an essential control is missing from the flow data. That is treatment with iKAT5 alone. Data should not be presented as fold change in percentage as it appears all cells still remain positive for PDGFR α . It seems that there is an increase in mean fluorescence intensity. For reference, the authors should include a negative control. Western blotting for protein amount, might also shed some light on whether the receptor is endocytosed and still present or if there is a loss of protein.
6. Does the observed reduction in PDGFR α affect the signaling of this pathway?
7. Data for F R1Q10 should be presented as % of positive cells. Not FAP area/cell. The "resting" cells do not appear to be spread on the plate. Analyses should be performed when cells have attached for the same period of time.
8. Images in panel C of R2Q1 suggest that all cells are alpha smooth muscle actin positive. Again, Western blotting would provide a better understanding of the amount of asma than ICC. The number of replicates for the TH1834 +TGF β treatment is not readily apparent.
9. In general, current guidelines suggest that data should not be presented as fold change for experiments other than gene expression. The authors should consider presenting actual data points rather than normalized where feasible.
10. The authors should not use the term fibrosis for any of the in vitro results. They are simply looking at different fibroblast state. Not fibrosis.
11. The authors should consider listing potential limitations of their conclusions and experiments.

Open Access This Peer Review File is licensed under a Creative Commons Attribution 4.0 International License, which permits use, sharing, adaptation, distribution and reproduction in any medium or format, as long as you give appropriate credit to the original author(s) and the source, provide a link to the Creative Commons license, and indicate if changes were made.

In cases where reviewers are anonymous, credit should be given to 'Anonymous Referee' and the source.

The images or other third party material in this Peer Review File are included in the article's Creative Commons license, unless indicated otherwise in a credit line to the material. If material is not included in the article's Creative Commons license and your intended use is not permitted by statutory regulation or exceeds the permitted use, you will need to obtain permission directly from the copyright holder.

To view a copy of this license, visit <https://creativecommons.org/licenses/by/4.0/>

REVIEWER COMMENTS

Reviewer #1 (Remarks to the Author):

Aguado-Alvaro et al. aims to characterize the role of chromatin factors in fibroblast differentiation and implicating Tip60 as a pro-fibrotic factor by demonstrating that its inhibition can be used as a therapeutic approach for cardiac fibrosis. By developing a platform to functionally study fibrotic regulators, following up with Perturb-seq, and performing functional assays, the authors uncover numerous epigenetic regulators involved in fibrosis. The work, in general, displays how high throughput approaches in combination with rigorous functional assessment can identify and confirm chromatin factors and pathways involved in cardiac fibrosis providing potential therapeutic targets. However, there is a lack of validation regarding guide and Kat5 inhibitor efficiency and some of the data is not super convincing or has a small effect. Additionally, more mechanistic work could be done to display how human cardiac fibroblasts compare to the findings identified in this paper. Overall, the manuscript needs significant revision to be acceptable for publication.

We thank the reviewer for the constructive feedback, which has helped us to improve the clarity and rigor of our manuscript. The comments regarding guide validation, Kat5 inhibitor efficiency, and the strength of some of the data are well taken, and we have taken steps to address these concerns.

We have now added further validations for the CRISPR guides and Kat5 inhibitor, including Indel-seq to confirm the efficiency of the guides and Western blot and Immunofluorescence data to confirm protein downregulation following Kat5 inhibition. Additionally, we have re-analyzed datasets such as ATAC-seq results in murine CRISPRed cardiac fibroblasts and provided more detailed findings, including new control groups and experimental replicates where effects initially appeared less convincing.

To address the point about human cardiac fibroblasts, we have expanded our study by comparing our *ex vivo* murine data with human single-cell expression patterns of cardiac fibroblasts obtained from different clinical conditions reported in the literature. We also assessed, by performing bulk RNA-seq, the fibrotic response in patient-derived fibroblasts treated with the KAT5 inhibitor. Furthermore, we have provided more mechanistic work in cardiac fibroblasts isolated from patients and treated with the KAT5 inhibitor, supporting its anti-fibrotic effect. All these results enhance the translational relevance of our findings, demonstrating the therapeutic potential of KAT5 inhibition in human cardiac disease.

Please find our detailed responses to each of the reviewer's questions below:

Major points

1. While the authors cite that PDGFR α can be used to distinguish resting vs. fibrotic populations in humans and mice (line 119), it would be good to demonstrate this using human cardiac fibroblasts to make this finding more relevant to disease.

We thank the reviewer for this comment and agree that demonstrating that PDGFR α is also a good readout of resting states in human cardiac fibroblasts is of particular relevance. Concerning this issue, we want to point out that several studies have shown PDGFR α downregulation in human cardiac fibroblasts isolated from pathological cardiac tissue¹⁻³. Chaffin *et al.*¹ reported that PDGFR α is downregulated in transitions towards pathogenic states in human cardiac fibroblasts isolated from patients with dilated (DCM) and hypertrophic cardiomyopathies (HCM). This analysis suggests that PDGFR α downregulation is a hallmark of the fibroblast activation process in distinct human cardiomyopathies and that this marker could be used to distinguish naïve (higher levels of PDGFR α marker) from fibrotic fibroblasts (lower levels of PDGFR α marker) also in human cells (Fig. R1).

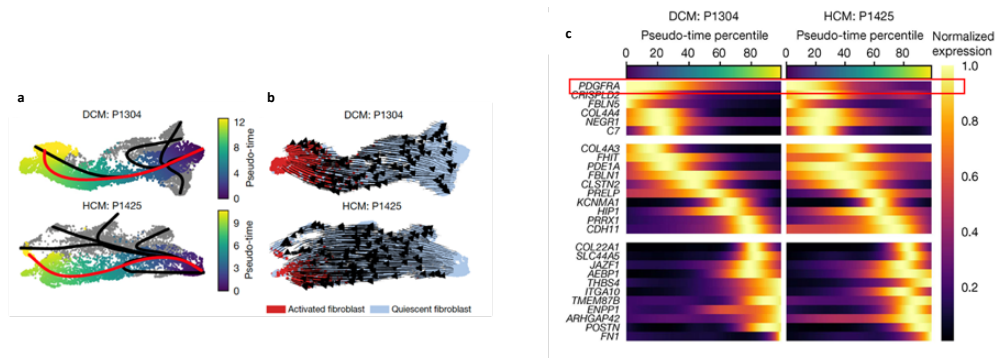


Figure R1 | DCM- and HCM-specific activated fibroblast populations downregulate PDGFRA. (a) UMAP representation of all fibroblasts from two patients (P1304: n=8,798 cells; P1425: n=7,164 cells) with overlaid Slingshot-inferred trajectories coloured by pseudo-time. The highlighted trajectory represents the most connected transition from quiescent to activated fibroblast. (b) UMAP representation with inferred RNA velocity overlaid as a stream plot. (c) Predicted expression of genes showing interesting patterns based on a negative binomial generalized additive model (NB-GAM) for each gene across pseudo-time in patient P1304 (left) and patient P1425 (right). Normalized expression is smoothed expression from NB-GAM scaled to the maximum value for each gene. PDGFRA gene is highlighted with a red square. Figure obtained from Fig. 3 from Chaffin *et al*¹.

Similarly, Koenig *et al.*² observed PDGFRA gene downregulation in fibroblasts obtained from DCM hearts compared to healthy donors. The table below (created based on the Supplementary Table 21 obtained from the article) shows this result:

Gene	log2FoldChange	padj
PDGFRA	-0,3464213557	0,01052755171

Amrute *et al.*³ also reported a decrease in PDGFRA gene expression when comparing cardiac fibroblasts isolated from heart failure patients to those obtained from healthy individuals. The table below (created based on the Supplementary Table 6 obtained from the article) shows this result:

Gene	log2FoldChange	padj
PDGFRA	-0,74937361	3,31E-06

Finally, to extend these findings, we performed flow cytometry to quantify PDGFR α expression in human cardiac fibroblasts (isolated from three patients who underwent cardiac surgery) cultured under three stimulated conditions: unstimulated, stimulated with TGF- β , and pre-treated with the KAT5 inhibitor (NU-9056) before TGF- β stimulation (Fig. R2). At baseline, PDGFR α expression was low, likely due to the already activated state of the fibroblasts analyzed. Upon TGF- β treatment, we observed further downregulation of PDGFR α , which was prevented with NU-9056 pre-treatment.

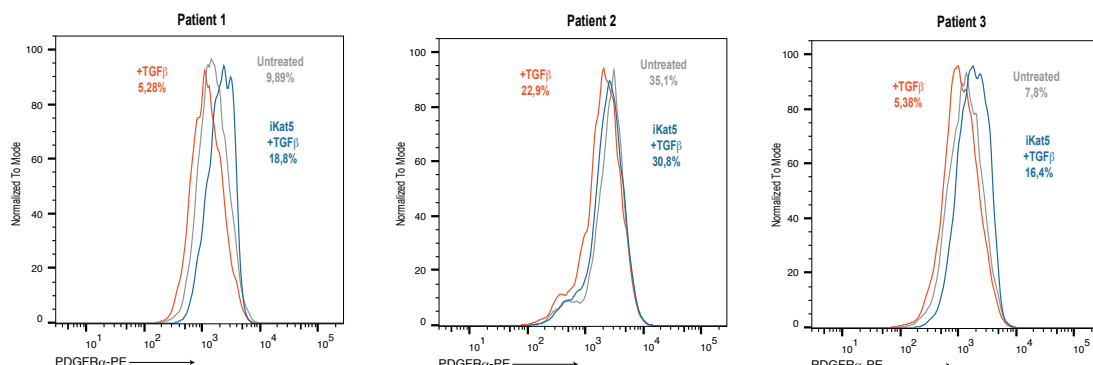


Figure R2 | FACS analysis for PDGFR α in human cardiac fibroblasts (obtained from three different patients undergoing cardiac surgery) in unstimulated (grey), TGF- β stimulated (red) and NU-9056 (5 μ M) pre-treated (blue) cells.

We believe these findings enhance the relevance of PDGFR α as a marker for distinguishing resting vs. fibrotic fibroblast populations in human cardiac pathology and support that KAT5 inhibition may help to maintain PDGFR α expression and mitigate fibroblast activation.

2. In Fig 1f, the authors use CRISPR to ablate TGFBR1 and SMAD4, but there is no clear validation that these guides produce a knockout using sequencing, PCR, or, ideally, western blot. Additionally, there is no clear validation of the guides used in Fig 2e or Fig 7g either. Extended Data Fig 5 may be showing this information at the RNA level, but if so, it is not clarified in the text or methods and Kat5, among others, is not convincing.

We thank the reviewer for raising this important point. To address this point, we have performed Indel-seq and Western blot analysis to confirm the genetic perturbation of the main targets in our study.

Indel-seq. We have amplified sgRNA target sites and performed deep sequencing analysis to detect insertions and deletions (indels) of nucleotides. The analyzed targets are *Tgfb1*, *Smad4*, *Kat5*, *Kat8*, *Srcap*, *Hcfc1* and *Wdr82*, in mice, and *KAT5* in human cardiac fibroblasts. Our results show indels formation at the target loci (Fig. R3) only in Cas9 expressing fibroblasts. These results are now included in Extended Data Fig. 1i (for *Smad4*- and *Tgfb1*-sgRNAs), Extended Data Fig. 7a (for *Wdr82*-, *Srcap*-, *Kat8*-, *Hcfc1*- and *Kat5*-sgRNAs), and Extended Data Fig. 10f (for human *KAT5*-sgRNA).

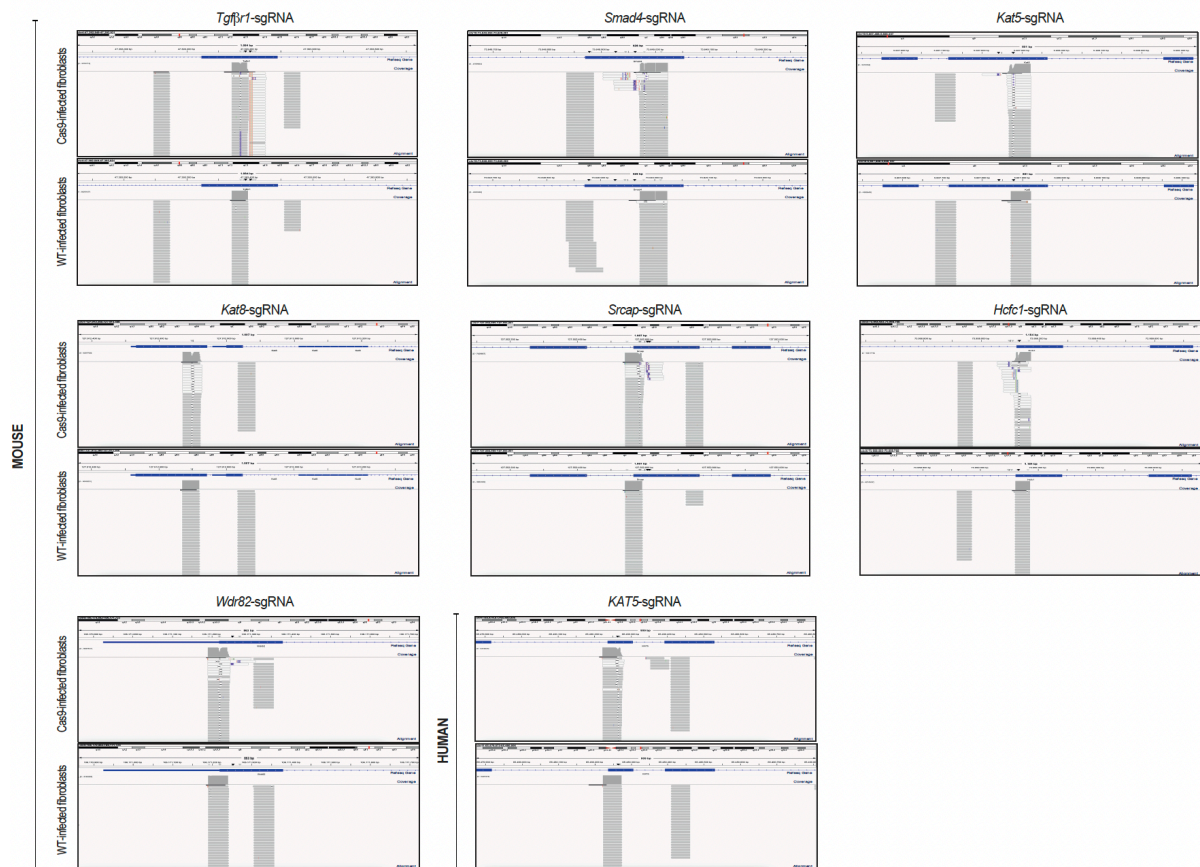


Figure R3 | Genome browser snapshots of Indel-seq signal for *Tgfb1*, *Smad4*, *Kat5*, *Kat8*, *Srcap*, *Hcfc1*, *Wdr82* (mouse) and *KAT5* (human) loci in Cas9 and wildtype (WT) murine and human cardiac fibroblasts transduced with *Tgfb1*-, *Smad4*-, *Kat5*-, *Kat8*-, *Srcap*-, *Hcfc1*-, *Wdr82*- (mouse), or *KAT5*- (human) sgRNAs.

Western blot analysis of *Tgfb1*, *Smad4* and *Kat5* protein levels. Results were normalized by quantifying the total protein loaded in the blot using Revert 700 total protein staining (LI-COR). We observed relevant downregulation of these proteins in CRISPR-edited Cas9 cardiac fibroblasts compared to controls (Fig. R4a-c), confirming the efficacy of the sgRNAs used at a protein level. These

results are now included in Extended Data Fig. 1j (for *Smad4*- and *Tgfb β 1*-sgRNAs) and Extended Data Fig. 7b (*Kat5*-sgRNA). Uncropped versions of blots (for both total and target proteins) can be found in Supplementary Fig. 2.

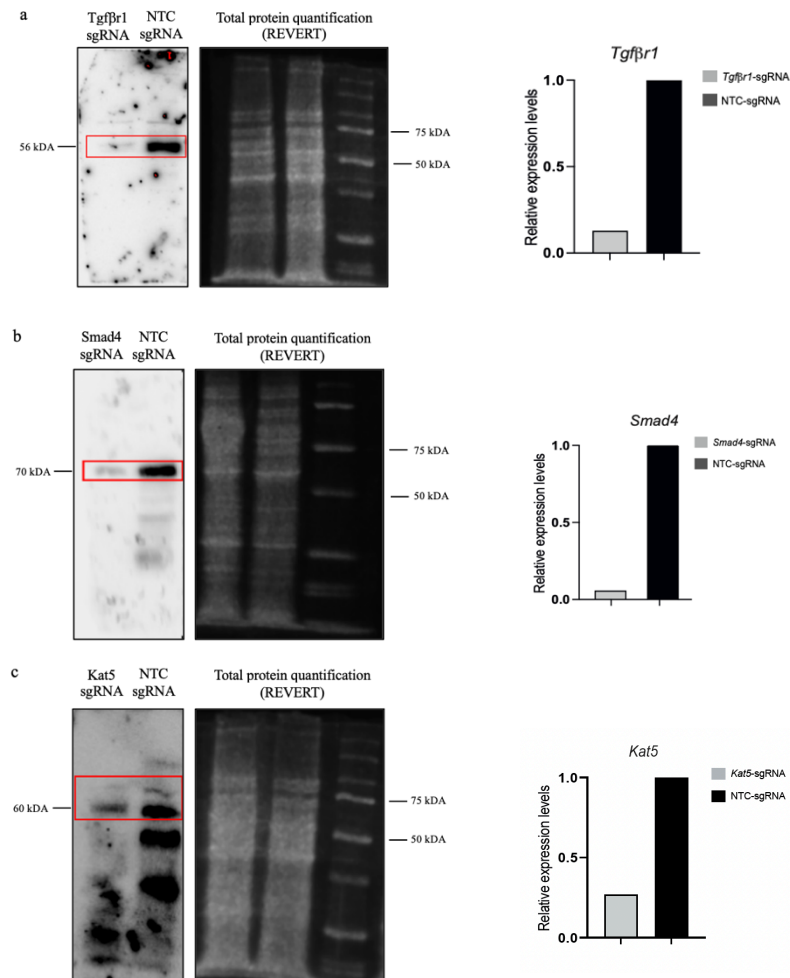


Figure R4 | Western blot of mouse *Smad4* (a), *Tgfb β 1* (b) and *Kat5* (c) proteins in Cas9 fibroblasts transduced with the target-gene or control (NTC) sgRNAs. Relative expression levels were calculated using total protein content loaded in the blot stained with Revert700 as a normalization factor.

It is important to note that protein quantification correlates with the percentage of infected (BFP⁺) cardiac fibroblasts used for protein extraction. A small percentage of cells were not transduced with the guides and thus continued expressing the target proteins. Specifically, 88.6% of cells were infected (BFP⁺) with *Tgfb β 1*-sgRNA, 92.4% with *Smad4*-sgRNA and 71.1% with *Kat5*-sgRNA (Fig. R5a-c). The remaining 11.4%, 7.6% and 28.9% of non-transduced cells explain the partial protein expression observed in the Western blot analysis.

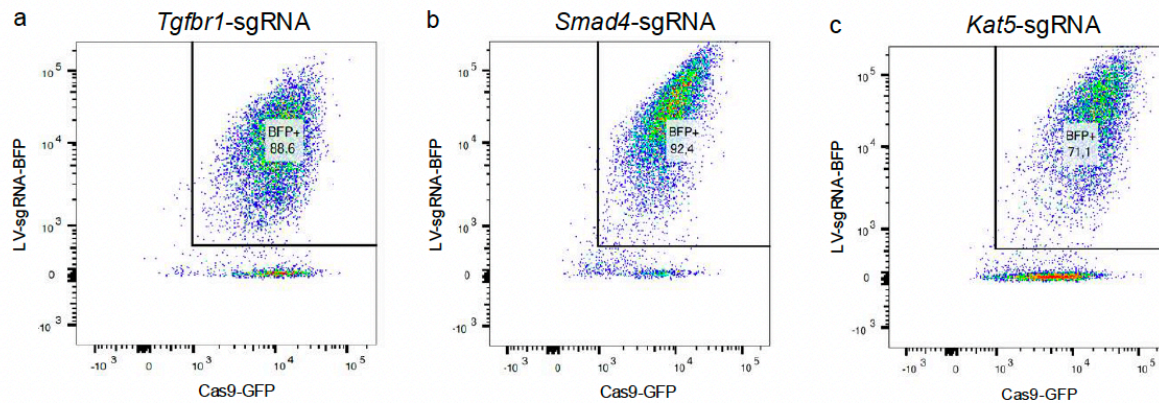


Figure R5 | Flow cytometry quantification of BFP⁺ percentage in Cas9-GFP cardiac fibroblasts infected with *Tgfbf1* (a), *Smad4* (b) and *Kat5* (c) sgRNAs.

3. In Fig 2c, it is not clear how a “fibrotic score” is generated. Fig 2a shows that NGS sequencing was performed to determine guide abundance in the two populations. Is this population enrichment termed “fibrotic score”? Additionally, “proliferation score” is not explained in the text and is not very relevant to the findings of the paper so should be omitted or moved to supplement.

We appreciate the reviewer’s observations and agree that additional clarification is needed regarding how the "fibrotic score" is generated.

The "fibrotic score" was determined by comparing the sgRNA abundance ratios between PDGFR α -high and PDGFR α -low populations. These ratios were calculated using deep sequencing data from previously FACS-isolated populations. This score indicates the relative enrichment of specific sgRNAs between the two groups, helping to identify epigenetic regulators whose disruption affects fibrotic pathways. We have now made this clearer in the manuscript (see Results section, page 3, paragraph 2, lines 124-129).

The "proliferation score", now termed as "viability score", was calculated by comparing the sgRNA distributions between Cas9 and non-Cas9 (wildtype) populations (including both PDGFR α -low and PDGFR α -high cells). This score was used to identify epigenetic regulators whose perturbation did not compromise the fitness of cardiac fibroblasts, a potential consideration for therapeutic targeting. However, we agree with the reviewer that this score is not essential to the primary findings of the manuscript. Therefore, we have moved the “viability score” from panel "d" of Fig. 2 (now Fig. 1) to a supplementary figure (Extended Data Fig. 2a) to streamline the presentation of our key results.

Both scores were calculated from two independent replicates of the screen. First, sgRNA counts were normalized against mean counts from NTC sgRNAs using the geometric mean, and the sgRNA-level log₂-fold enrichment/depletion was calculated using normalized sgRNA counts comparing two paired screens of interest (i.e., Cas9 vs. wildtype, or Fibrotic vs. Naïve). The replicates were also used to calculate a p-value via 2-sided *t*-test. Then, to calculate gene-level scores from sgRNA-level log₂-fold changes and p-values, we took the median over sgRNAs that target the same genes and *p*-values were combined using the Fisher method. Finally, the Benjamini-Hochberg false discovery rate (FDR) was applied to calculate corrected p-values for the 726 genes tested. This more detailed explanation of how both scores were obtained can be found in the Methods section “Computational analysis of FACS-based CRISPR screens” (page 13, paragraph 1, lines 606-615) and is also provided in the caption of revised Fig. 1c.

4. Functional validation assays are very convincing. It would be nice to see the images for the

collagen secretion assay, if available. Additionally, more rationale could be provided for why these specific assays were chosen.

We appreciate the reviewer's thoughtful feedback. Collagen secretion was quantified using an ELISA assay, so we do not have corresponding images available. However, we agree that it is important to clarify the rationale behind selecting these specific assays. These specific functional assays were chosen to link the transcriptional results observed in our Perturb-seq approach with key functional processes mediated by fibrotic fibroblasts. This rationale is now explained in the manuscript (Results section, page 5, paragraph 2, line 219-221). Additionally, these assays are widely accepted and have been used by other research groups to confirm the activation and differentiation of cardiac fibroblasts into myofibroblasts in studies of both murine models⁴ and human cells⁵, which we now cite.

5. Better peaks could be used for Fig 6a. In particular, *Myl9* and *Meox1* are not super convincing. This data would be better if quantified.

We appreciate the reviewer for highlighting this point. We agree that the peaks shown in Fig. 6a (now Fig. 4a) were not very convincing. To address this, we have improved the resolution of the image and zoomed in on the peaks that demonstrate the clearest changes in chromatin accessibility. Furthermore, we have substituted the peaks shown for *Myl9* with a peak for *Mmp13* (also involved in fibrosis), which shows a more convincing change (Fig. R6a). Additionally, we would like to clarify that the samples shown in Fig. 6a (now Fig. 4a) are the merged of 2 independent samples from different ATAC-seq experiments, so we have also included a figure (Fig. R6b) with the peaks of the individual samples of each replicate in Extended Data Fig. 8a, to provide clarity and robustness to the presentation of these findings.

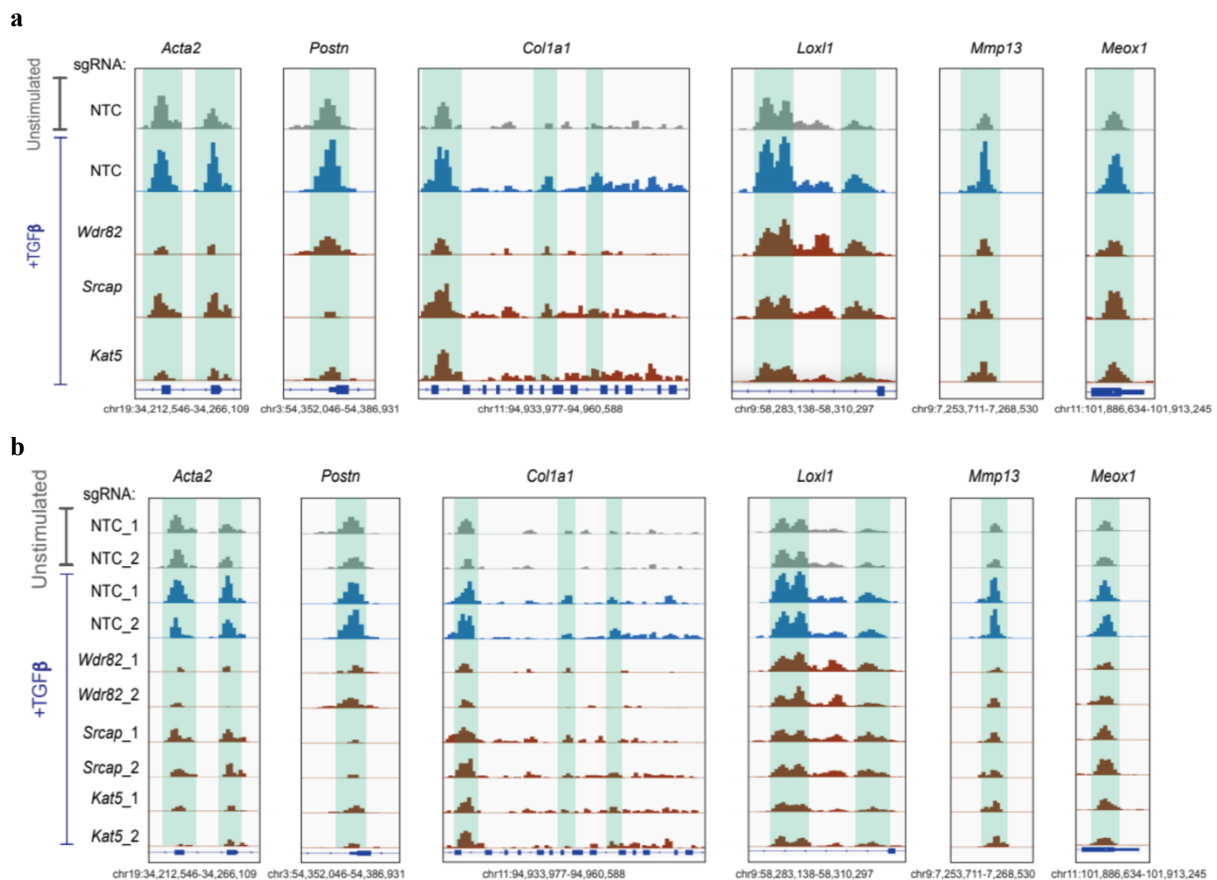


Figure R6 | Genome browser snapshots of ATAC-seq signal for fibrotic loci in cardiac fibroblasts: unstimulated (grey), 24h TGF-β-stimulated (blue) and *Wdr82*, *Srcap* and *Kat5* knockouts in TGF-β stimulated conditions (red). Peaks for the merged (a) or individual two replicate (b) samples of each condition are shown.

6. Kat5 chemical inhibitor was not validated by looking at RT-qPCR for changes in Kat5 gene expression. This should be added to Fig 7b as validation.

We agree on the importance of validating the activity of the Kat5 inhibitor (NU-9056). To validate Kat5 inhibition, we have assessed the acetylation levels of H2AZ, its main substrate, using immunofluorescence analysis. We have included data quantifying H2AZ acetylation levels in murine (Extended Data Fig. 8j,) and human (Extended Data Fig. 10b) cardiac fibroblasts following TGF- β stimulation, both with and without pre-treatment with NU-9056. Our results show a decrease in H2AZ acetylation in NU-9056 treated fibroblasts, providing clear evidence that NU-9056 effectively inhibits Kat5 activity in both species (Fig. R7). Of note, H2AZ acetylation levels increase by around 10-fold in murine cardiac fibroblasts stimulated with TGF- β , which reinforces the link between TGF- β /fibrosis and H2AZ acetylation. This pattern is not recapitulated in patient-derived fibroblasts, and we believe this is due to the pre-activated/fibrotic state of patient-derived fibroblasts (likely caused by their fibrotic origin).

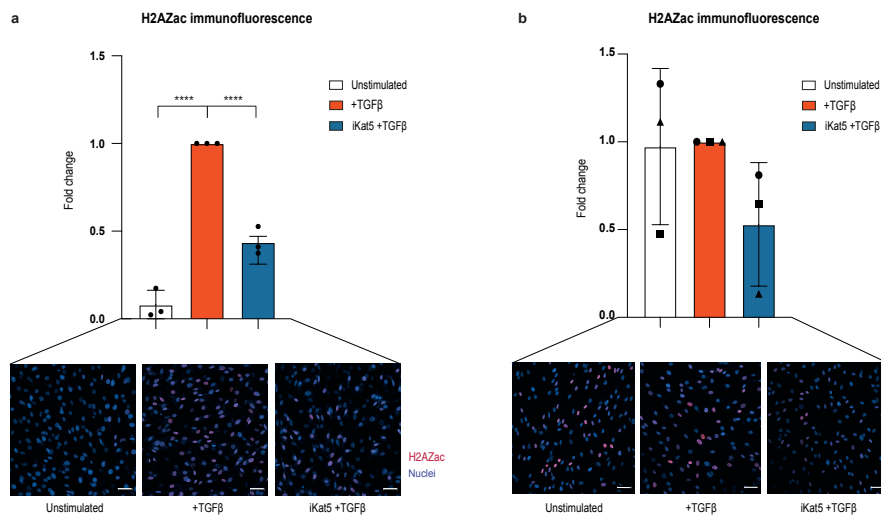


Figure R7 | Kat5 inhibition attenuates H2AZ acetylation levels in murine and human primary cardiac fibroblasts. (a) Quantification of the percentage of H2AZac positive cells, following TGF- β stimulation in control and NU-9056 pre-treated murine cardiac fibroblasts. The measurements were derived from three replicate experiments. **(b)** Quantification of the percentage of H2AZac positive cells, following TGF- β stimulation in control and NU-9056 pre-treated human cardiac fibroblasts. The measurements were derived from three patients who underwent cardiac surgery. Each patient is represented by a different symbol. Representative images of H2AZac immunostaining assays are shown at the bottom. Scale bars: 50 μ m. Statistical significance was analyzed by one-way ANOVA test. ****P < 0.0001. All data are shown as fold change vs. TGF- β values and are mean \pm SD.

7. Fig 7d is not convincing given the scale of the differential binding score. It would also be beneficial to see accessibility in iKat5 + TGFB and Mock + TGFB treated cells via browser tracks for Tead 1-4.

We acknowledge the reviewer's comment that the size-effects in the original ATAC-seq analysis were not convincing. In response, we conducted additional replicates to generate more robust data, which are now included in the revised version of the manuscript (Fig. 4j). Cardiac fibroblasts pre-treated with the Kat5 chemical inhibitor (NU-9056) before TGF- β stimulation show strong changes in accessibility of Tead and Cebp TF motifs, which recapitulates the pattern observed upon genetic perturbation of Kat5 (Fig. R8).

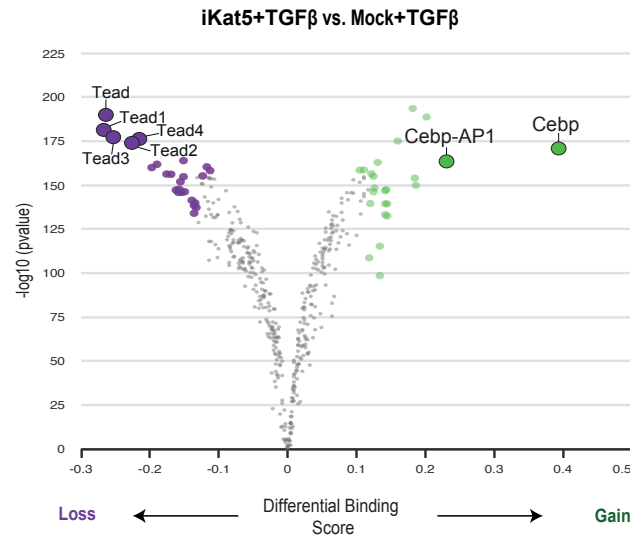


Figure R8 | Decreased Tead and increased Cebp motifs accessibility. Differential TF-footprinting analysis between control (vehicle/mock) and NU-9056 pre-treated murine fibroblasts after TGF- β stimulation. Dots in purple represent TF motifs with decreased accessibility in NU-9056 pre-treated murine fibroblasts and dots in green represent TF motifs with gained accessibility.

Regarding reviewer's request to present browser tracks for Tead 1-4 in iKat5+TGF- β and Mock+TGF- β treated cells, we would like to clarify that the analysis has identified changes in the accessibility of Tead motifs across the genome. In other words, we have measured the accessibility across all potential Tead binding sites (motifs) not at the specific Tead loci.

8. Overall, Fig 7a-e would benefit from an unstimulated control so the readers can see how iKat5 treated cells and control cells compare.

We appreciate the reviewer's suggestion to include unstimulated controls in Fig. 7. In response, we conducted three additional experiments with an unstimulated control condition, and the results have been integrated into the revised Fig. 4g, as shown below. The inclusion of the unstimulated control highlights how the gene expression levels of key fibrotic genes return to near-baseline levels in fibroblasts pre-treated with Kat5 inhibitor (Fig. R9).

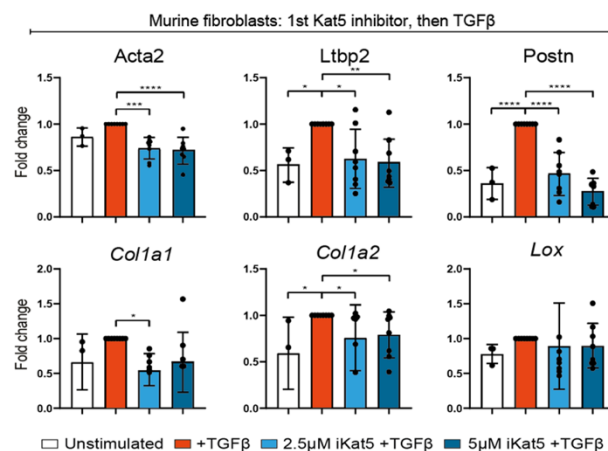


Figure R9 | Kat5 inhibition attenuates fibrotic responses in murine cardiac fibroblasts. Relative expression ($2^{-\Delta\Delta CT}$) of fibrotic marker genes in unstimulated control (vehicle) or following TGF- β stimulation in control (vehicle) and NU-9056 pre-treated murine cardiac fibroblasts. The measurements were performed in three-eight replicate experiments. Statistical significance was analyzed using one-way ANOVA or Kruskal-Wallis tests. * $P < 0.05$, ** $P < 0.01$, *** $P < 0.001$, **** $P < 0.0001$. All data are mean \pm SD.

For the reversion experiments in Fig. 7e (now Extended Data Fig. 8k), we explored the potential of Kat5 inhibitor to revert the fibrotic phenotype induced by TGF-β treatment. Since the goal was to examine the reversal of fibroblast differentiation following stimulation, we believe including unstimulated controls in this context would not provide additional insight.

9. Fig 7f-h is very promising. It would improve the impact of the paper to expand this data to a full figure. Additional experiments could be done including the three assays done in Fig 5 as well as ATAC-seq on the unstimulated, TGFB, and iKat5 + TGFB treated cells. Likewise, it would be highly impactful if the authors could show that isolated human cardiac fibroblasts with heart failure have a similar phenotype to the TGFB or IL1B treated cells and adding iKat5 reverses some of the cardiac fibrosis.

We appreciate the reviewer’s suggestion to expand the data presented in Fig. 7f-h. Given the promising results obtained in human cardiac fibroblasts, we have expanded this data into a full figure (Fig. 6 and Extended Data Fig. 10) and conducted additional experiments to further substantiate our findings.

First, we cross-referenced our *ex vivo* single-cell expression patterns with the single-cell expression patterns of human cardiac fibroblasts isolated from hearts in different clinical conditions^{1–3,6,7} (Fig. R10a). This analysis showed a clear correlation between our *ex vivo* murine fibroblast states and clinically relevant human cardiac subpopulations. For instance, our *ex vivo* naïve fibroblasts were related to human fibroblast subpopulations characteristic of healthy myocardium and our *ex vivo* myofibroblasts were related to fibrotic subpopulations of fibroblasts that appear in failure hearts from patients with myocardial infarction (MI) or Dilated (DCM), Hypertrophic (HCM) or Arrhythmogenic (ARVC) cardiomyopathies (Fig. R10b).

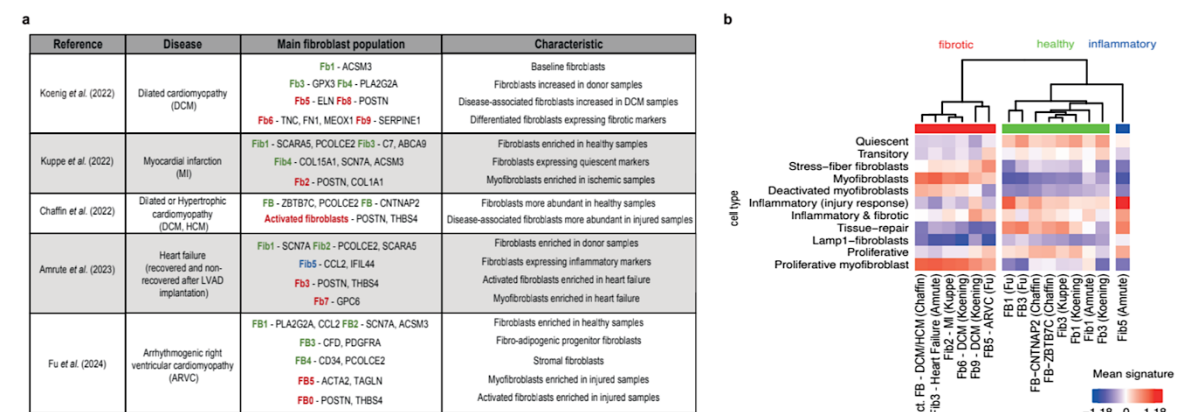


Figure R10 | *Ex vivo* single-cell expression patterns of murine cardiac fibroblasts are related to *in vivo* single-cell expression patterns of human cardiac fibroblasts. (a) Table summarizing key papers used for human signature comparisons conducted with the *ex vivo* murine data. **(b)** Enrichment of *in vivo* fibroblast expression signatures from references in **(a)** over *ex vivo* fibroblast populations from this study.

In addition, this analysis shows that depletion of some of our candidate targets (including *Kat5*, *Srcap* or *Wdr82*, and our positive control *Smad3*) in our *ex vivo* murine fibroblasts downregulated gene expression signatures specific of human fibrotic fibroblasts found in pathological conditions and, conversely, upregulated healthy fibroblast signatures (Fig. R11).

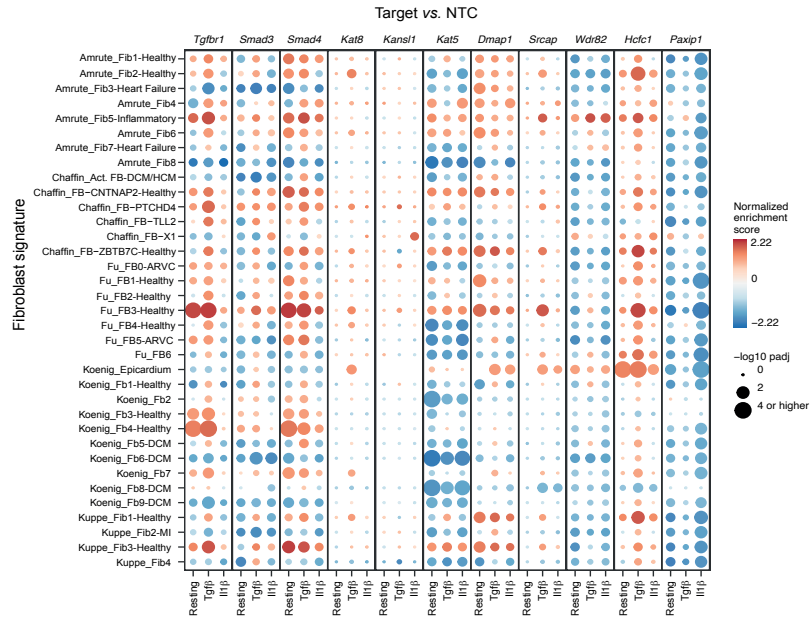
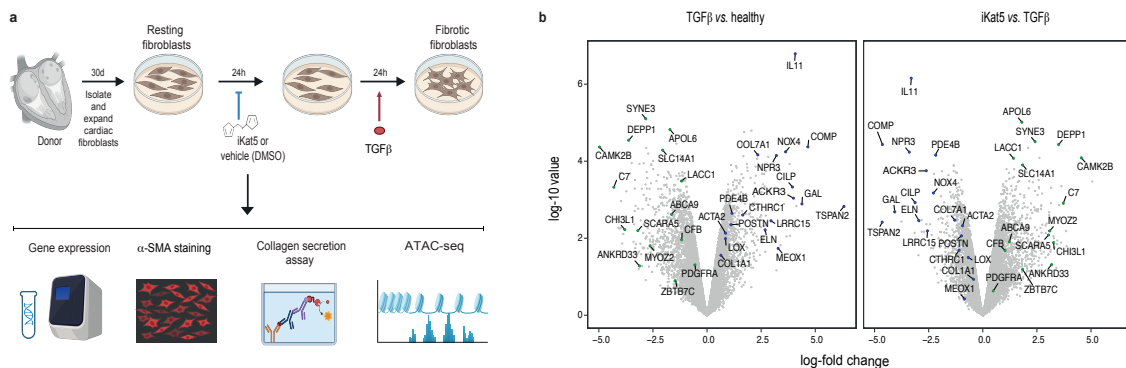


Figure R11 | Gene set enrichment analysis of differentially expressed genes across representative knockouts. Fibroblast expression signatures are taken from references in Fig. 10a. The color of each dot represents normalized enrichment score, the size represents the $-\log_{10}$ adjusted p-value.

Taken together, these results suggest a functional conservation (human-mouse) of the transcriptional regulators that orchestrate cardiac fibrotic responses. These results are part of the reviewed manuscript Fig.6a-b and Extended Data Fig. 10a.

Then, using RNA-seq, we analyzed the expression patterns of patient-derived cardiac fibroblasts pre-treated with vehicle or KAT5 inhibitor before TGF- β stimulation (Fig. R12a). TGF- β treatment induced a marked fibrotic response in unperturbed (vehicle) human cardiac fibroblasts characterized by the upregulation of typical hallmark fibrosis markers including POSTN, CTHRC1, ACTA2 (α -SMA) (Fig. R12b). Pre-treatment with KAT5 inhibitor reduced the fibrotic response to TGF- β , pushing cardiac fibroblasts back to a healthy (unstimulated) state (Fig. R12b-d). Furthermore, patient-derived fibroblasts pre-treated with KAT5 inhibitor downregulated the transcriptional signatures characteristic of pathological human fibroblast subpopulations described above (Fib2-Kuppe, Fib6,8-9-Koenig, Act_FB-Chaffin, Fib3-Amrute, FB0-Fu) (Fig. R12e). These results were confirmed using genetic perturbation (CRISPR) of *KAT5* and qPCR measurements of four key fibrotic genes (Fig. R12f-g).



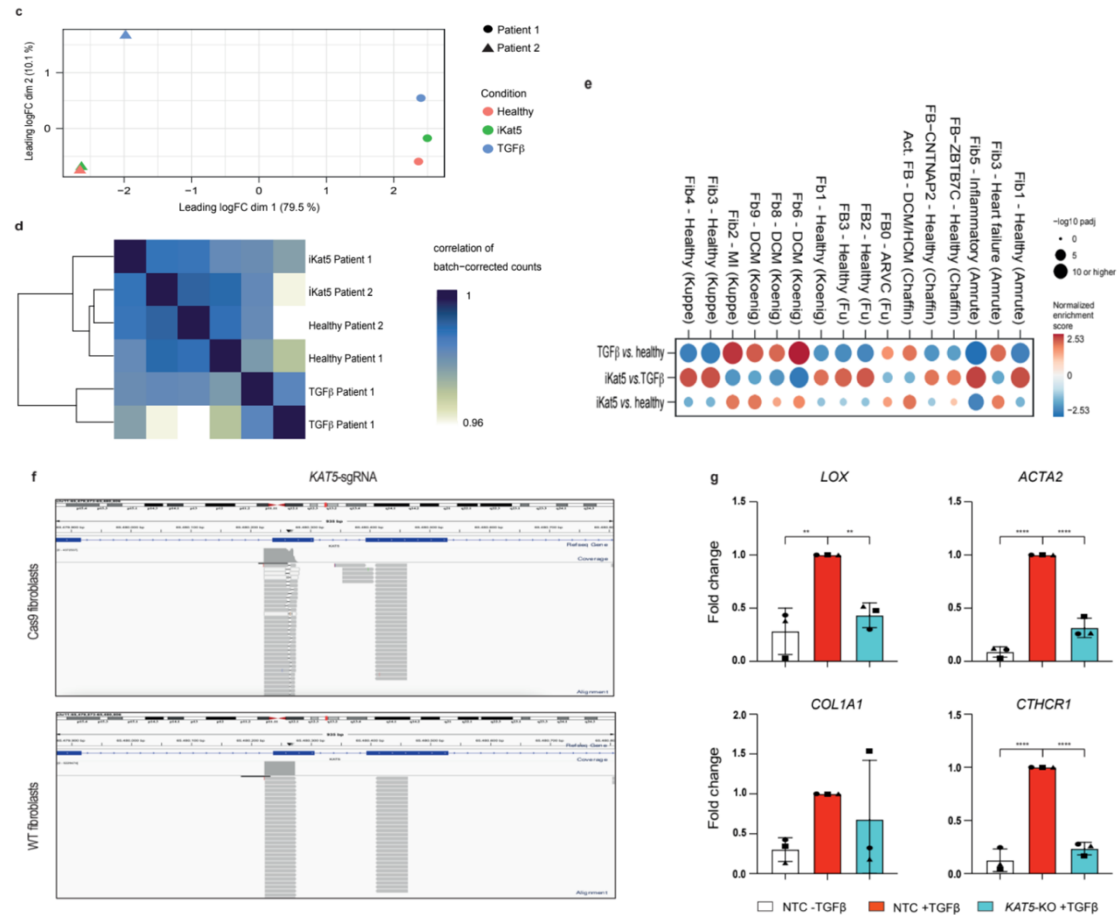


Figure R12 | KAT5 chemical and genetic perturbations attenuate fibrotic responses in human primary cardiac fibroblasts. (a) Schematic depiction of the experimental approach in human cardiac fibroblasts. (b) Differentially expressed markers of fibrosis in TGF- β -treated patient-derived cardiac fibroblasts (left) and in fibroblasts pre-treated with KAT5 inhibitor before the TGF- β stimulus (right). (c) Principal component analysis of gene expression in patient-derived cardiac fibroblasts. Dimension 1 corresponds to variability of gene expression between patients, while dimension 2 captures effects of TGF- β or KAT5 inhibitor on the transcriptome. (d) Correlation analysis of gene expression demarcates samples treated with TGF- β from unstimulated and KAT5-inhibited samples. (e) Gene set enrichment analysis of differentially expressed genes across treatments. Fibroblast expression signatures are taken from references in Fig. R10a. The color of each dot represents normalized enrichment score, the size represents the $-\log_{10}$ adjusted p-value. (f) Genome browser snapshots of Indel-seq signal for *KAT5* loci in Cas9 and wildtype (WT) human cardiac fibroblasts transduced with *KAT5*-sgRNA. (g) Gene expression analysis ($2^{-\Delta\Delta CT}$) of fibrotic markers in human cardiac fibroblasts depleted for KAT5 using CRISPR/Cas9 and then stimulated with TGF- β . The measurements were performed in cell cultures from three different patients. Each patient is represented by a different symbol. Statistical significance was analyzed by one-way ANOVA test. ** $P < 0.01$, **** $P < 0.0001$. All data are mean \pm SD.

In addition, we measured stress-fiber formation and collagen deposition in patient-derived fibroblasts pre-treated with KAT5 inhibitor. These functional assays were conducted following 24 hours of TGF- β stimulation in control (vehicle) and NU-9056 (5 μ M) pre-treated human fibroblasts isolated from three different patients. The results show that KAT5 inhibition substantially reduces α -SMA protein levels and collagen secretion, providing direct evidence of its anti-fibrotic effects in human samples (Fig. R13a-b).

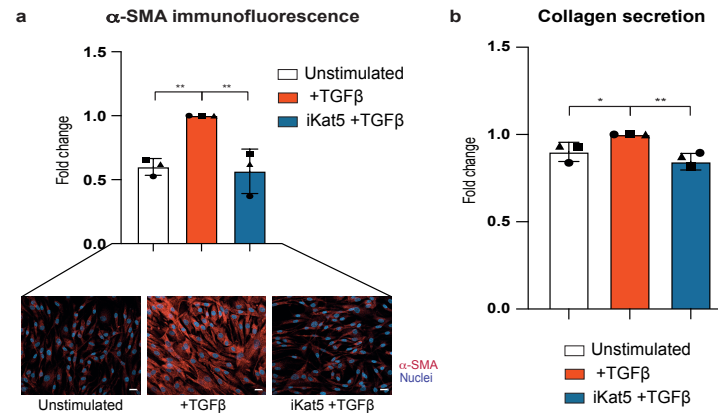


Figure R13 | KAT5 inhibition attenuates fibrotic responses in human primary cardiac fibroblasts. (a) Quantification of the average immunofluorescence intensity of α -SMA, following TGF- β stimulation in control and NU-9056 pre-treated human cardiac fibroblasts. The measurements were derived from three patients. Representative images of α -SMA immunostaining assays are shown at the bottom. Scale bars: 20 μ m. (b) Quantification of collagen secretion following TGF- β stimulation in control (vehicle) and NU-9056 pre-treated human cardiac fibroblasts. The measurements were performed in three patients. Each patient is represented by a different symbol. Statistical significance was analyzed by one-way ANOVA test. * $P < 0.05$, ** $P < 0.01$. All data are shown as fold change vs. TGF- β values and are mean \pm SD.

Finally, we analysed the chromatin accessibility patterns of patient-derived cardiac fibroblasts pre-treated with KAT5 inhibitor before TGF- β stimulation. This experiment showed a striking similarity with the murine results, where TEAD TF motifs showed a clear downregulation in their chromatin accessibility in human cardiac fibroblasts pre-treated with KAT5 inhibitor (Fig. R14). The strong similarity between human and mouse ChrF-TF dependencies suggests that the epigenetic mechanisms regulating fibrotic transformation in cardiac fibroblasts are conserved in mammals.

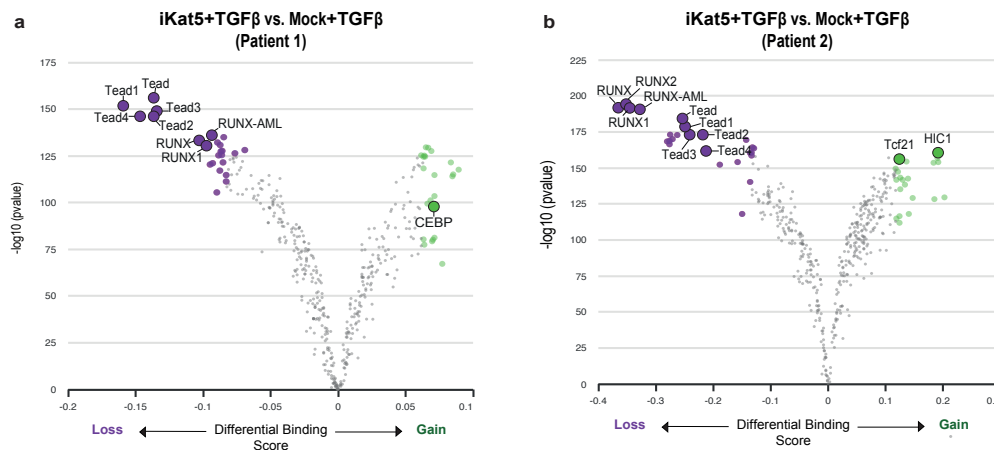


Figure R14 | Differential TF-footprinting analysis between control (vehicle) and NU-9056 pre-treated human fibroblasts after TGF- β stimulation. Dots in purple represent TF motifs with decreased accessibility in NU-9056 pre-treated human fibroblasts. Dots in green represent TF motifs with increased accessibility in NU-9056 pre-treated human fibroblasts. Patient 1 (a) and Patient 2 (b) are shown.

In conclusion, these results reinforce our findings suggesting KAT5 inhibition as a potential therapeutic avenue to alleviate cardiac fibrosis and have been included in revised Fig. 6c-h and Extended Data Fig. 10c-g.

10. As the introduction highlights, “myocardial fibrosis is a frequent outcome of many cardiac pathologies.” As such, many studies have shown fibroblast activated protein (FAP) induced by both TGFb and IL-1B treatment *in vitro*, which population in the scRNA experiment is marked by FAP expression, and do any of the perturbations affect its expression?

We thank the reviewer for this relevant question. We examined FAP expression across the different conditions and populations identified in the scRNA-seq experiment (Fig. R15a-b) and evaluated its levels following the perturbation of various chromatin factors (Fig. R15c). However, we observed that the expression of FAP remained consistently low in all experimental conditions, i.e. we only detected few reads in few cells and the gene was actually removed by standard scRNA-seq pre-processing tools. We thus conclude that FAP expression was below the limit of detection of the scRNA-seq technology.

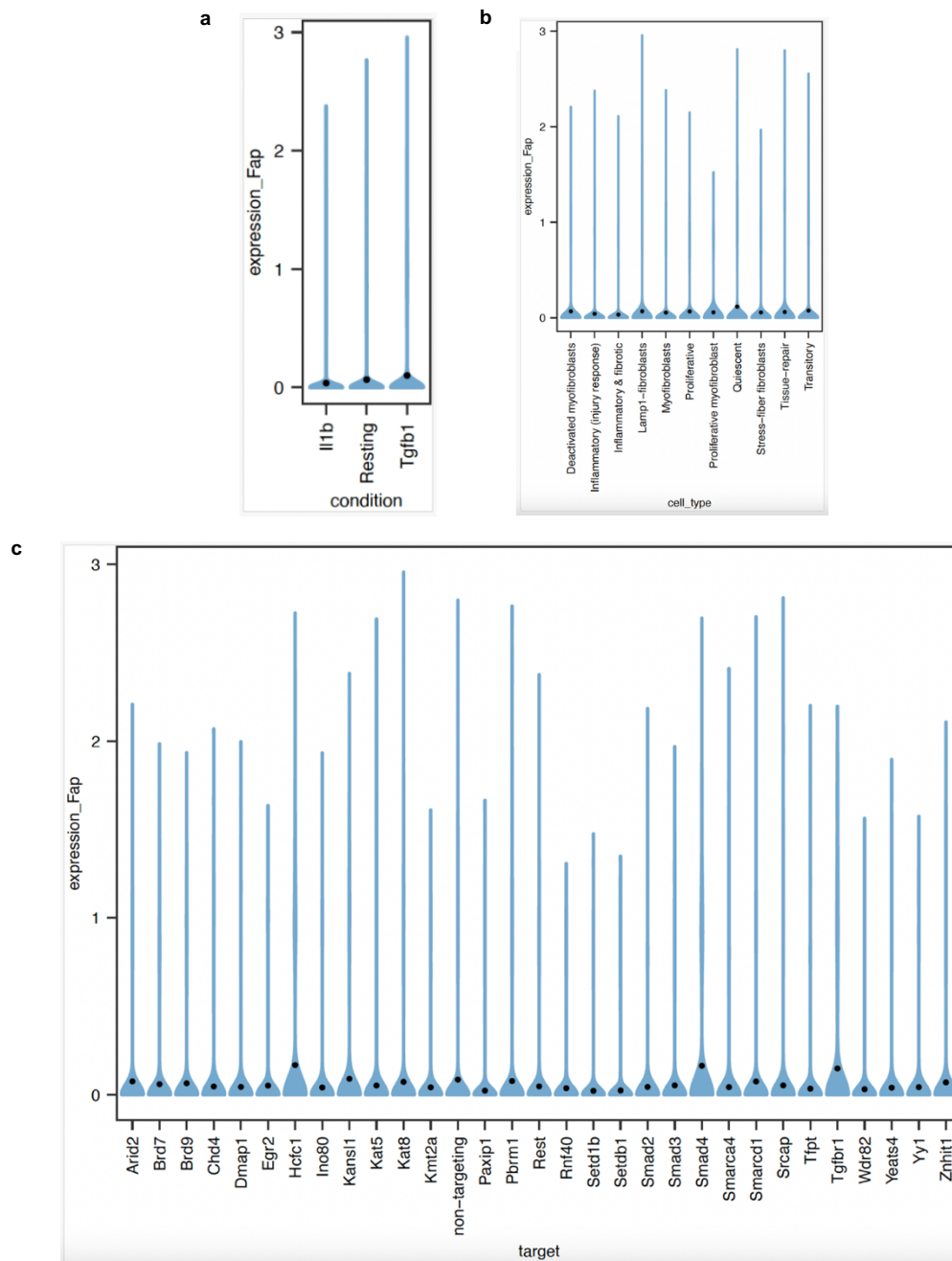


Figure R15 | Log-counts per million normalized expression of Fap in Perturb-seq data across (a) conditions, (b) fibroblast subtypes, and (c) CRISPR targets. Black dots denote mean expression.

Minor points

1. The abbreviation of chromatin factors as CF is very confusing since many people use CF as an abbreviation for cardiac fibroblasts. I would recommend changing this.

We agree that using “CF” as an abbreviation for chromatin factors could lead to confusion, as “CF” is commonly used to refer to cardiac fibroblasts. To avoid ambiguity, we have replaced “CF” with “ChrF” throughout the manuscript.

2. Serum-free expansion and selection of FACS marker data can all be in the supplement since it is methodological and not super relevant to the findings of the paper (Figure 1). It makes more sense to start the paper on the CRISPR screen.

We agree that the data on serum-free expansion and FACS marker selection is more methodological and less central to the paper’s main findings. As a result, Fig. 1 has been moved to the supplemental section and merged with Extended Data Fig. 1.

3. Text size on Fig 3a should be increased to improve readability.

We thank the reviewer for this suggestion. The text size on Fig. 3a (now Fig. 2a) has been adjusted to improve readability and ensure clarity.

4. It is not clear how many replicates were performed for the Perturb-seq screen since the data is not displayed by replicate via UMAP.

Since the focus of the paper is the study of fibrosis we chose to perform 4 replicates for resting conditions, 4 replicates for TGF- β and 2 replicates for IL-1 β . However, one of the TGF- β replicates rendered low data quality and it was removed from the analysis (Fig. R16). To clarify how many replicates were performed for the Perturb-seq screen we have included this panel in the Extended Data Fig. 2b.

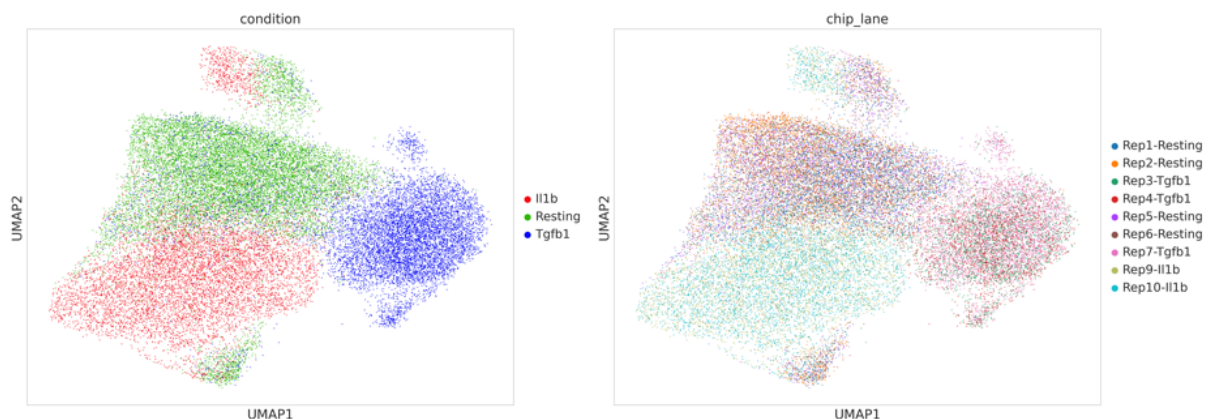


Figure R16 | UMAP projections showing cultured conditions (left) and replicates (right) for Perturb-seq screens performed in this study.

5. Fig 5c represents 2 biological replicates with 50 technical replicates. I would like to clarify that the Kruskal-Wallis test was conducted comparing the 2 values for each condition as opposed to 100 technical replicate values because of the high level of significance.

We appreciate the reviewer’s request for clarification. The results presented in Fig. 5c (now Fig. 3d) were obtained from two independent biological replicates, with 50 individual cell measurements per experiment. The graphs display all 100 cell measurements combined. The Kruskal-Wallis test was applied to the complete dataset, considering the combined cell measurements across both replicates.

6. Fig 5e-f can be moved to supplement.

We thank the reviewer for the suggestion. Fig. 5e-f (now Extended Data Fig. 7c-d) has been moved to the supplementary section to streamline the main text and focus on the core findings.

7. Fig 7a shows the Kat5 inhibitor was applied for 7 days while the text (Line 320) says 24 hours. Please clarify.

We apologize for the oversight. The correct duration of Kat5 inhibitor treatment is 24 hours, as mentioned in the text (line 320). Fig. 7a (now Fig. 4f) has been corrected to reflect this, ensuring consistency between the figure and the text.

Reviewer #2 (Remarks to the Author):

In this manuscript, the Authors aimed to identify and characterize the chromatin factors influencing fibroblast differentiation and their role in cardiac fibrosis. They conducted CRISPR screens on mouse cardiac fibroblast cells treated with TGF- β to pinpoint SRCAP, TIP60, NSL complex, HCFC1, and WDR82 as potent regulators of fibrotic states with specific readout (PDGFR α). Subsequently, the Authors investigated the effects of depleting these factors on three key processes driving fibrotic transformation: collagen deposition, stress-fiber formation, and contractility. They validated their findings using an *in vitro* fibrosis model. Additionally, the Authors employed ATAC-seq profiling and differential TF footprinting analysis to establish connections between these chromatin factors and the chromatin accessibility of pro-fibrotic transcription factors. Finally, they utilized a KAT5-specific chemical inhibitor (NU-9056) on murine and human cardiac fibroblasts, demonstrating its potential for therapeutic development. The manuscript is well written and figures are well prepared.

We thank the reviewer for the positive feedback on our manuscript. We are pleased that our work has been well-received, and we hope that the additional results we now provide further strengthen the translational relevance of Kat5 inhibition and offer a more comprehensive understanding of its effects in both *in vitro* and *in vivo* models.

Following are the major issues needs to be addressed to reach the conclusion of manuscript:

1. The experiments were solely conducted *in vitro* using fibroblast cells stimulated with TGF- β . It's essential for the Authors to verify whether the findings of the manuscript are specific to cardiac fibroblast cells or applicable to fibroblast cells from other sources – a general or specific. Experimental validation using fibroblast cells isolated from other organs is required to address this question.

We thank the reviewer for raising this important point. It is indeed important to assess whether the effects of Kat5 inhibition are specific to cardiac fibroblasts or extend to fibroblasts from other organs, particularly since fibroblasts play essential roles in tissue repair and fibrosis across various organs.

To address this, we performed *in vitro* functional analyses using fibroblasts isolated from murine lungs, skin, and kidneys. We first confirmed the fibroblast phenotype of these cells by flow cytometry, ensuring they expressed fibroblast markers (MEFSK4, CD90, CD73, CD44, CD29), and were negative for other cell types, such as pericytes (CD146, NG2), endothelial cells (CD31, CD34), and hematopoietic cells (CD45). This confirmed the purity of the fibroblast populations used in the subsequent experiments (Fig. R17a-c).

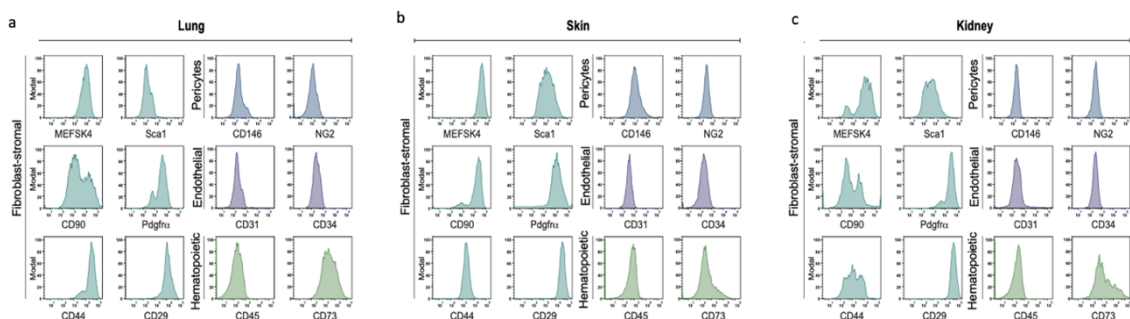


Figure R17 | Characterization of primary murine lung, skin and kidney fibroblasts. (a-c) Representative FACS analysis of fibroblast (MEFSK4, CD90, CD73, CD44, CD29), pericytes (CD146, NG2), endothelial (CD31, CD34) and hematopoietic (CD45) cell markers in unstimulated lung (a), skin (b) and kidney (c) fibroblasts at day 7 of culture (n=3).

Upon treating these fibroblasts with the Kat5 inhibitor (NU9056) (Fig. R18a), a strong downregulation of fibrotic hallmark genes was observed in lung fibroblasts, with milder effects in skin and kidney

fibroblasts, as seen through qPCR and α -SMA protein expression (Fig. R18b-g). Additionally, collagen secretion was significantly reduced in lung fibroblasts and only mildly decreased, albeit without statistical significance, in skin and kidney derived fibroblasts (Fig. R18h-j). These findings suggest that Kat5 inhibition effectively mitigates fibroblast activation and fibrosis in multiple organs, with the strongest effects found for cardiac and lung fibroblasts. This broadens the therapeutic relevance of Kat5 inhibition as a potential strategy for mitigating fibrosis across various tissues.

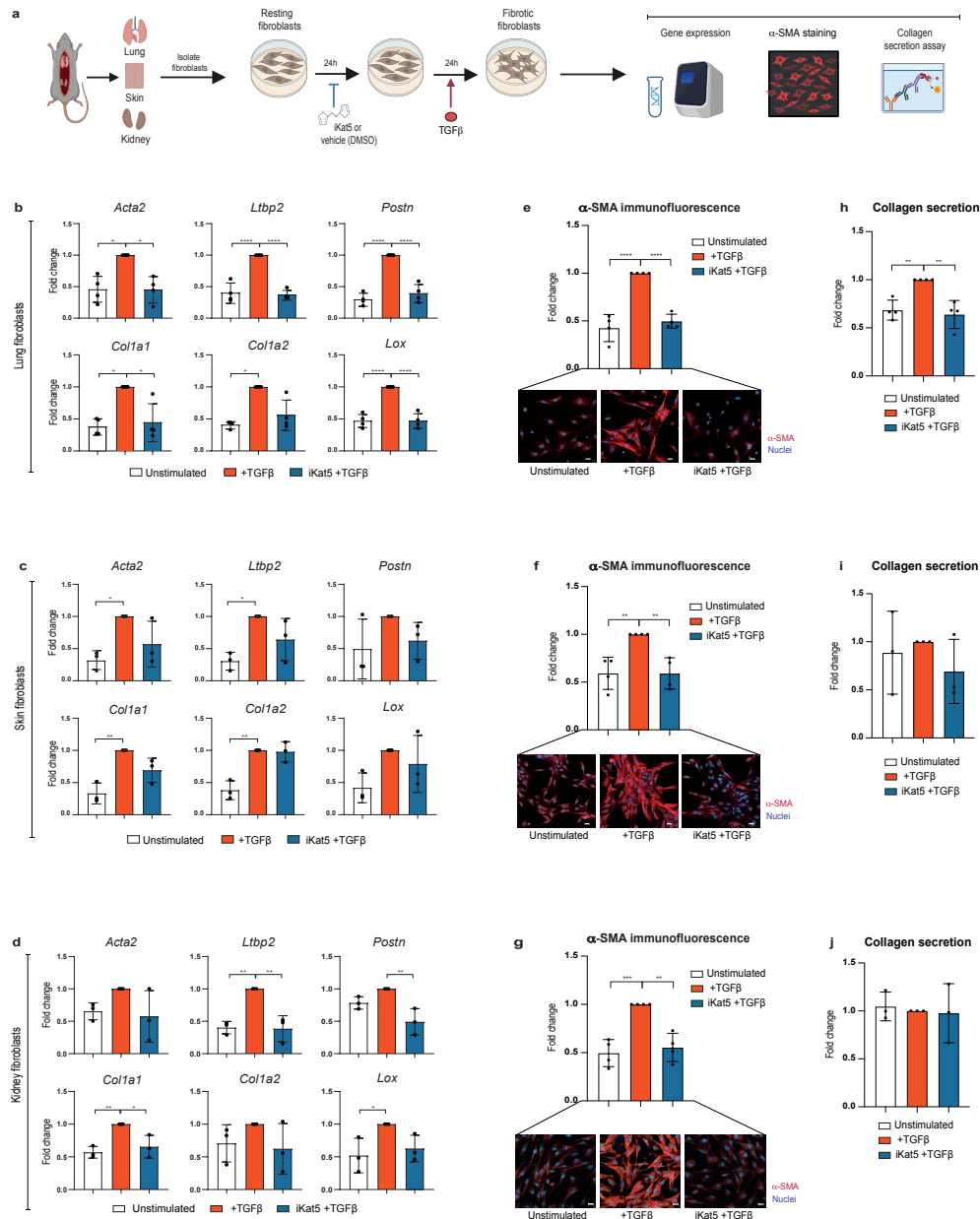


Figure R18 | Kat5 inhibition attenuates fibrotic responses in murine primary fibroblasts. (a) Schematic depiction of the experimental approach in murine lung, skin and kidney fibroblasts. (b-d) Relative expression ($2^{-\Delta\Delta CT}$) of fibrotic marker genes in unstimulated control (vehicle) or following TGF- β stimulation in control (vehicle) and NU-9056 (5 μ M) pre-treated murine lung (b), skin (c) and kidney (d) fibroblasts. The measurements were performed in three-four replicate experiments. (e-g) Quantification of the average immunofluorescence intensity of α -SMA, following TGF- β stimulation in control and NU-9056 pre-treated murine lung (e), skin (f) and kidney (g) fibroblasts. The measurements were performed in four replicate experiments. Representative images of α -SMA immunostaining assays are shown at the bottom. Scale bars: 20 μ m. (h-j) Quantification of collagen secretion following TGF- β stimulation in control and NU-9056 pre-treated murine lung (h), skin (i) and kidney (j) fibroblasts. The measurements were performed in three replicate experiments. Statistical significance was analyzed by one-way ANOVA or Kruskal-Wallis tests. * $P < 0.05$, ** $P < 0.01$, *** $P < 0.001$, **** $P < 0.0001$. All data are shown as fold change vs. TGF- β values and are mean \pm SD.

These results are now included in Fig. 5 of the revised manuscript.

2. In figures 7a-e, the authors treated primary fibroblast cells isolated from murine cardiac tissue with a KAT5-specific chemical inhibitor followed by TGF-B treatment to demonstrate its prophylactic protective effect. To claim therapeutic relevance, experiments should be conducted in a therapeutic setup both *in vitro* and *in vivo*, utilizing a fibrotic murine model.

We agree with the reviewer that *in vivo* evaluation of Kat5 inhibition is crucial to better understand its therapeutic potential for treating fibrotic diseases.

To address this, we have initiated experiments using a murine model of myocardial infarction (MI). Adult mice (10 weeks old) were subjected to permanent ligation of the left descending coronary artery as previously described by our group⁸, and groups of 7-9 mice were treated with either NU-9056 Kat5 inhibitor (10 mg/kg) or DMSO vehicle as a control starting 3 days post-MI and continued daily for 21 days. Cardiac function was assessed by echocardiography (Vevo 3100 imaging system) at day 2 and day 30 post-infarction (Fig. R19a). NU-9056-treated mice demonstrated improved cardiac remodeling, with stable diastolic and systolic volumes and areas one month post-MI, unlike the vehicle-treated controls, which showed significant heart dilation (Fig. R19b).

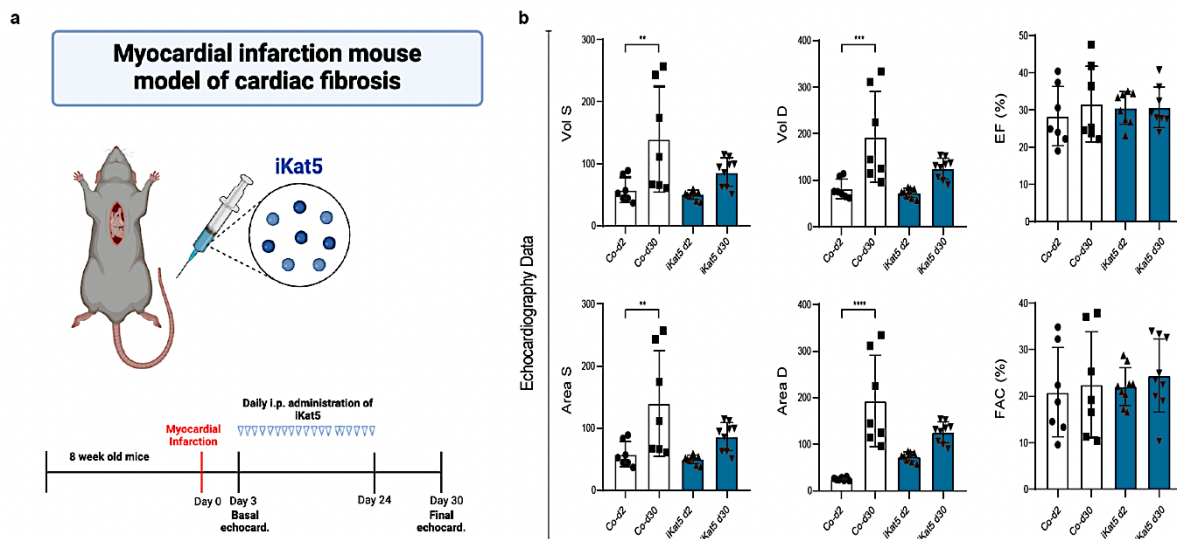


Figure R19 | Administration of Kat5 chemical inhibitor NU-9056 preserves cardiac deleterious remodeling after MI. (a) Schematic depiction. Echocardiography studies were performed at day 2 (basal) and day 30 (final) post-MI in mice daily treated with NU-9056 (10 mg/kg) (or vehicle), beginning on day 3 after MI, for 21 consecutive days. **(b)** Echocardiography data. Cardiac systolic (S) and diastolic (D) ventricle areas (mm²) and volumes (μL), ejection fraction (EF) (%) and fractional area change (FAC) (%) were measured. Statistical significance was calculated by ANOVA with multiple comparisons test between day 2 and day 30 post-MI and is represented as **P < 0.01, ***P < 0.001, and ****P < 0.0001. Data were obtained from 7-9 animals per group. Mean ± SD values are represented.

These results are promising but we have noticed that demonstrating the beneficial effects of Kat5 inhibition *in vivo* requires further optimization of Kat5 inhibitor delivery and a deep characterization of fibroblast dynamics during myocardial healing in infarcted animals. This represents a significant extension of the work presented in this paper. Given that we have already expanded significantly the study by incorporating: a) analysis of fibrotic responses in fibroblasts isolated from 3 other organs and b) a deep analysis of KAT5 inhibition in patient-derived fibroblasts, we feel that these *in vivo* studies fall beyond the scope of the current article.

It is worth noting that a different Kat5 inhibitor, TH1834, has been described in the literature⁹ and shown to be effective in a murine model of MI, improving systolic function and reducing cardiac apoptosis and fibrosis.

Furthermore, with respect to the *in vitro* studies, we would like to clarify that in Fig. 7e (now Extended Data Fig. 8k) we mimicked a therapeutic setup in mouse cardiac fibroblasts by first inducing a fibrotic phenotype using TGF- β stimulation followed by treatment with the Kat5 inhibitor (NU-9056). These experiments led to clear reversion of the fibrotic phenotype highlighting the potential of Kat5 inhibition to treat fibrotic conditions.

3. In figures 7f-h, primary fibroblast cells isolated from human cardiac tissue were treated with a KAT5-specific chemical inhibitor followed by TGF- β treatment to demonstrate its prophylactic protective effect. To establish therapeutic relevance, experiments should be conducted in a therapeutic setup, such as using fibroblasts isolated from human fibrotic heart tissue.

We appreciate the reviewer's suggestion and recognize the importance of establishing therapeutic relevance by using fibroblasts from human fibrotic heart tissue. However, we would like to clarify that the human cardiac fibroblasts used in our experiments are indeed derived from a therapeutic setup, as they were isolated from discarded cardiac tissue from patients with cardiac dysfunction. In fact, the pathological state of these patient-derived fibroblasts is reflected by low PDGFR α expression (quantified by flow cytometry, Fig. R20a), high H2AZac levels (quantified by IF, Fig. R20b) and moderate response to TGF- β stimulation, when compared to murine fibroblasts isolated from healthy hearts.

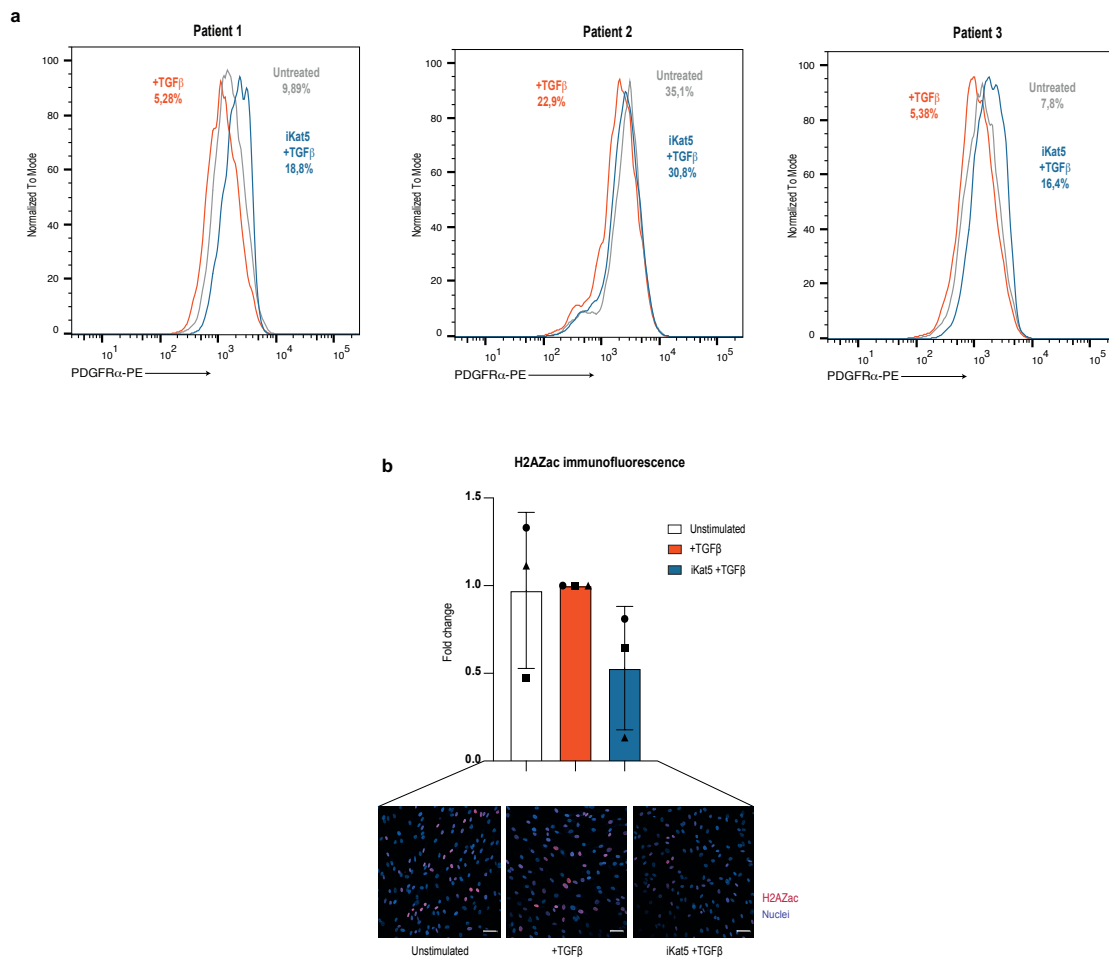
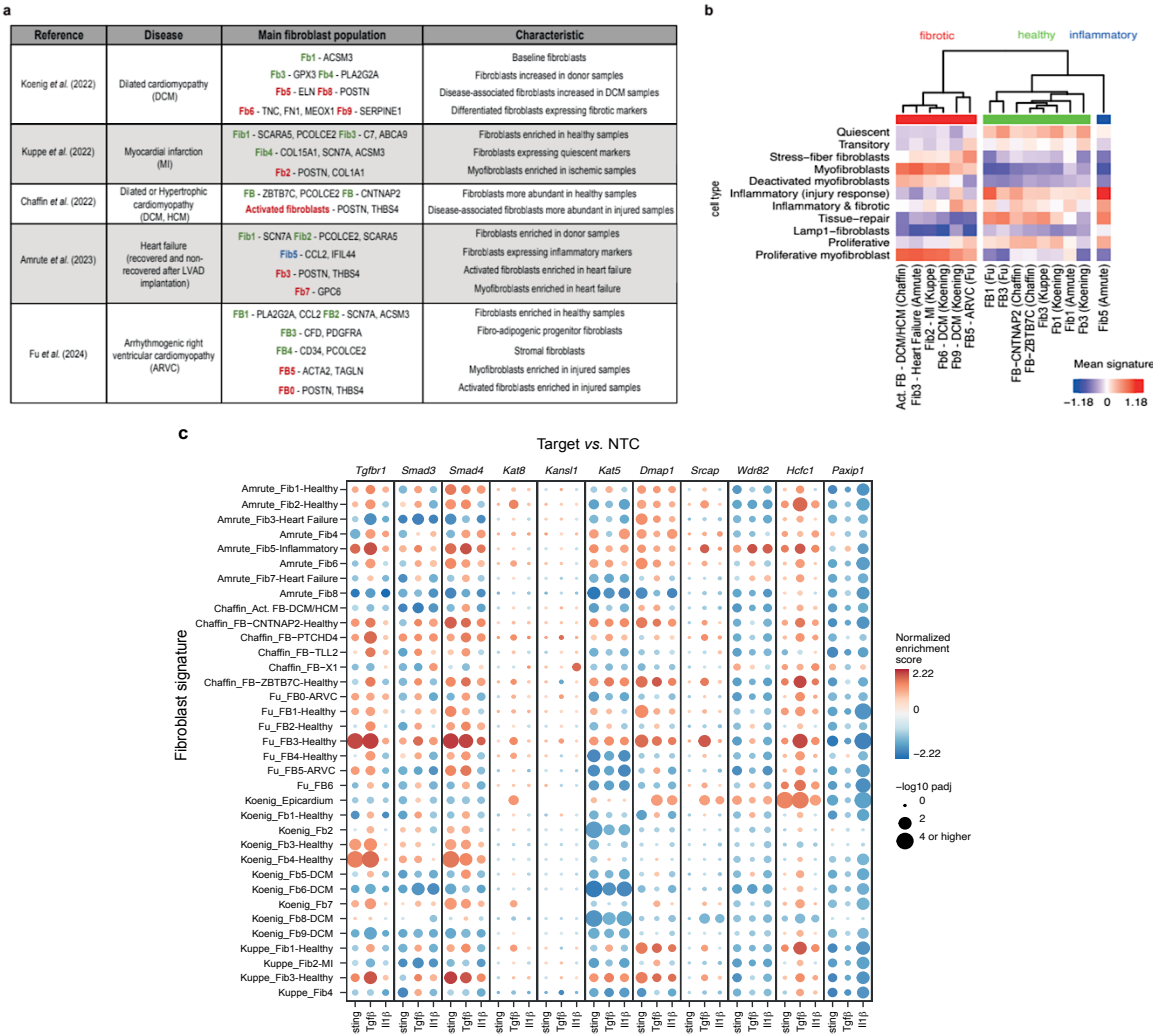


Figure R20 | Low expression of PDGFR α naïve marker and high levels of H2AZac epigenetic mark suggest the partially activated/fibrotic state of patient-derived cardiac fibroblasts used in this study even in the unstimulated/resting condition. (a) FACS analysis of PDGFR α marker in human cardiac fibroblasts obtained from three different patients undergoing cardiac surgery and culture under three stimulated conditions: unstimulated (grey), TGF- β stimulated (red) and NU-9056 (5 μ M) pre-treated (blue) cells. At baseline, PDGFR α expression was low, likely due to the already activated state of the fibroblasts analyzed. Upon TGF- β treatment, we observed further downregulation of PDGFR α , which was prevented with NU-9056 pre-treatment. **(b)** Quantification of the percentage of H2AZac positive cells in unstimulated control or following TGF- β stimulation control and NU-9056 pre-treated human cardiac fibroblasts. The measurements were derived from three

patients who underwent cardiac surgery. Each patient is represented by a different symbol. Representative images of H2AZac immunostaining assays are shown at the bottom. Scale bars: 50 μ m. Data is shown as fold change vs. TGF- β values and is mean \pm SD.

In addition to this clarification, we want to note that the updated manuscript includes a deeper examination of the anti-fibrotic effects of KAT5 inhibition in human-derived cardiac fibroblasts. These results are included in Fig. 6 and Extended Data Fig. 10 and are summarized below:

1. We have cross-referenced our *ex vivo* single-cell expression patterns with the single-cell expression patterns of human cardiac fibroblasts isolated from hearts in different clinical conditions^{1-3,6,7} (Fig. R21a). This analysis showed a clear correlation between our *ex vivo* murine fibroblast states and clinically relevant human cardiac subpopulations. For instance, our *ex vivo* naïve fibroblasts were related to human fibroblast subpopulations characteristic of healthy myocardium and our *ex vivo* myofibroblasts were related to fibrotic subpopulations of fibroblasts that appear in failure hearts from patients with myocardial infarction (MI) or Dilated (DCM), Hypertrophic (HCM) or Arrhythmogenic (ARVC) cardiomyopathies (Fig. R21b). This analysis also shows that depletion of our candidate target *Kat5* in our *ex vivo* murine fibroblasts downregulated gene expression signatures specific of human fibrotic fibroblasts found in pathological conditions (Fig. R21c).



data. **(b)** Enrichment of *in vivo* fibroblast expression signatures from references in (a) over *ex vivo* fibroblast populations from this study. **(c)** Gene set enrichment analysis of differentially expressed genes across representative knockouts, including *Kat5*. Fibroblast expression signatures are taken from references in (a). The color of each dot represents normalized enrichment score, the size represents the $-\log_{10}$ adjusted p-value.

- We have used RNA-seq to measure the fibrotic responses to TGF- β in patient-derived fibroblasts treated with KAT5 inhibitor (Fig. R22a). This showed a marked attenuation of the fibrotic responses highlighted by the downregulation of fibrotic signatures characteristic of cardiac fibroblast subpopulations found in pathological hearts: Fib2-Kuppe, Fib6,8-9-Koenig, Act_FB-Chaffin, Fib3-Amrute, FB0-Fu; and, conversely, the upregulation of healthy fibroblast signatures (Fig. R22b-e).

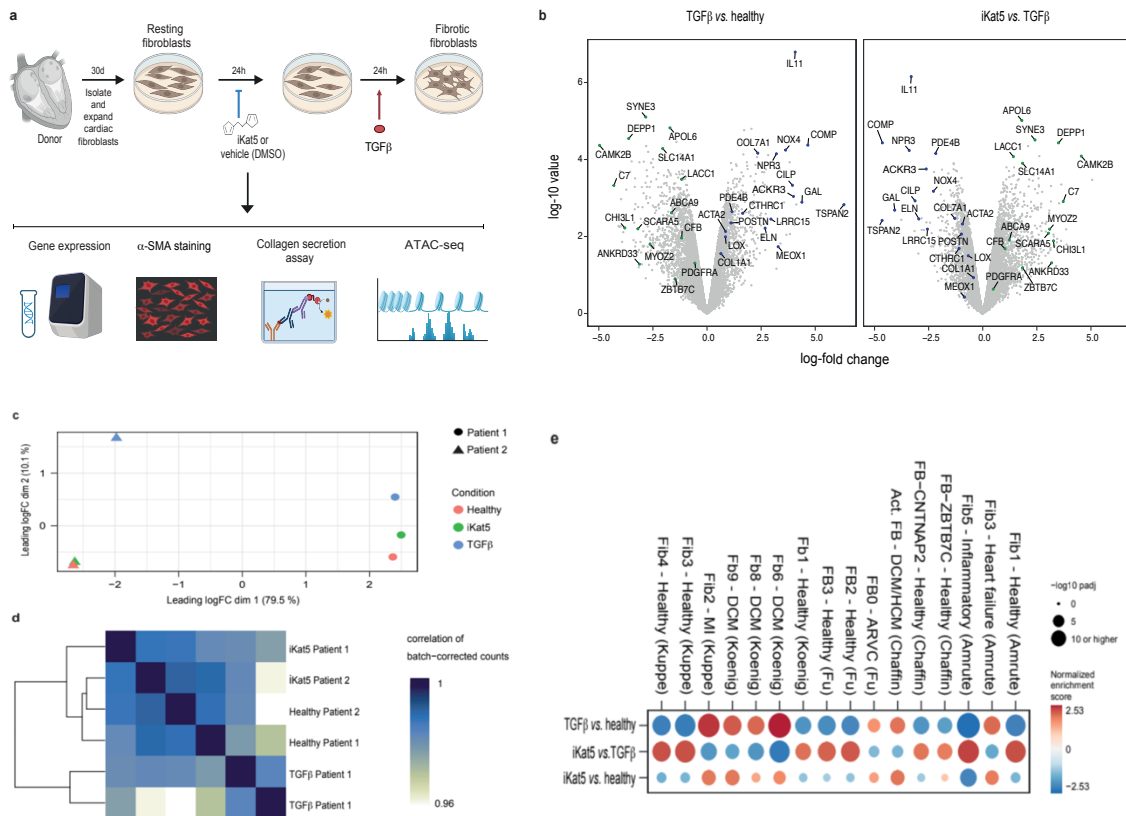


Figure R22 | KAT5 chemical inhibition attenuates fibrotic responses in human primary cardiac fibroblasts. (a) Schematic depiction of the experimental approach in human cardiac fibroblasts. **(b)** Differentially expressed markers of fibrosis in TGF- β -treated patient-derived cardiac fibroblasts (left) and in fibroblasts pre-treated with KAT5 inhibitor before the TGF- β stimulus (right). **(c)** Principal component analysis of gene expression in patient-derived cardiac fibroblasts. Dimension 1 corresponds to variability of gene expression between patients, while dimension 2 captures effects of TGF- β or KAT5 inhibitor on the transcriptome. **(d)** Correlation analysis of gene expression demarcates samples with TGF- β from unstimulated and KAT5-inhibited samples. **(e)** Gene set enrichment analysis of differentially expressed genes across treatments. Fibroblast expression signatures are taken from references in Fig. R21a. The color of each dot represents normalized enrichment score, the size represents the $-\log_{10}$ adjusted p-value.

- We show a clear reduction in stress-fiber formation and collagen secretion in patient-derived fibroblasts pre-treated with KAT5 inhibitor before TGF- β stimulation (Fig. R23a-b). These two fibrotic parameters were also decreased in unstimulated patient-derived fibroblasts treated with KAT5 inhibitor (Fig. R24a-b). These last results (Fig. R24a-b) are preliminary and require more replicates to confirm their statistical significance, therefore we have not included them in the manuscript, but we expect they will be useful to convince the reviewer of the clinical relevance of KAT5 inhibitor.

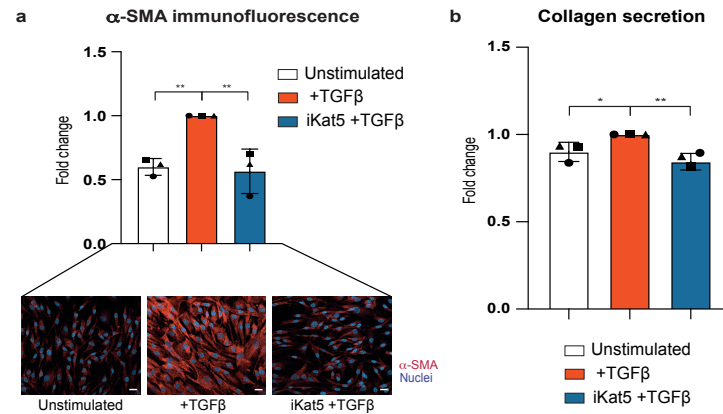


Figure R23 | KAT5 inhibition attenuates fibrotic responses in human primary cardiac fibroblasts. (a) Quantification of the average immunofluorescence intensity of α -SMA, following TGF- β stimulation in control (vehicle) and NU-9056 pre-treated human cardiac fibroblasts. The measurements were derived from three patients. Representative images of α -SMA immunostaining assays are shown at the bottom. Scale bars: 20 μ m. (b) Quantification of collagen secretion following TGF- β stimulation in control (vehicle) and NU-9056 pre-treated human cardiac fibroblasts. The measurements were performed in three patients. Each patient is represented by a different symbol. Statistical significance was analyzed by a one-way ANOVA test. * $P < 0.05$, ** $P < 0.01$. All data are shown as fold change vs. TGF- β values and are mean \pm SD.

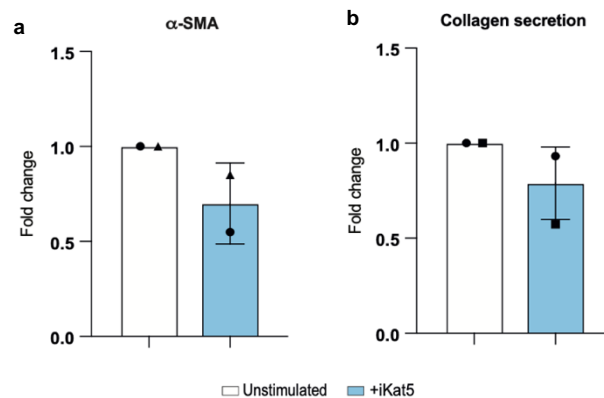


Figure R24 | KAT5 inhibition attenuates the fibrotic phenotype of unstimulated human primary fibroblasts isolated from patients with cardiac disease. (a) Quantification of the average immunofluorescence intensity of α -SMA, in control (vehicle) and NU-9056-treated unstimulated human cardiac fibroblasts. All the measurements were derived from two patients. (b) Quantification of collagen secretion in control (vehicle) and NU-9056-treated unstimulated human cardiac fibroblasts. The measurements were performed in two patients. Each patient is represented by a different symbol. All data are shown as fold change vs. Unstimulated values and are mean \pm SD.

- We have observed a strong similarity in the epigenetic status of patient-derived human and murine cardiac fibroblasts treated with KAT5 inhibitor (Fig. R25). In both cases, we observed a marked reduction of the accessibility of TEAD motifs in cells treated with KAT5 inhibitor. This highlights a strong conservation of the molecular mechanisms that mediate fibrotic transformation in mammals.

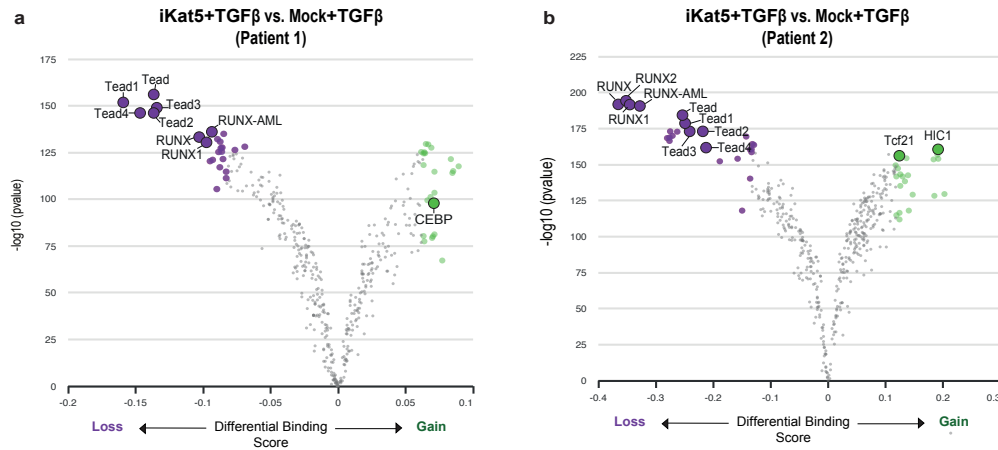


Figure R25 | Differential TF-footprinting analysis between control (vehicle) and NU-9056 pre-treated human fibroblasts after TGF- β stimulation. Dots in purple represent TF motifs with decreased accessibility in NU-9056 pre-treated human fibroblasts. Dots in green represent TF motifs with increased accessibility in NU-9056 pre-treated human fibroblasts. Patient 1 (a) and Patient 2 (b) are shown.

Minor issues:

1. Standardized nomenclature for Gene and Protein names should be rectified throughout the text. For instance, when referring to the protein KAT5, it should be capitalized consistently (line 314, 315).

We apologize for the typographical errors. The nomenclature has been standardized throughout the manuscript, ensuring consistent formatting of gene and protein names. Capitalized nomenclature is used exclusively when referring to the human (genes or proteins) and italic nomenclature when referring to genes (mouse and human).

Reviewer #3 (Remarks to the Author):

This article explores the role of epigenetic regulatory factors in cardiac fibroblasts during fibrogenesis. The study utilizes both bulk and single-cell CRISPR screening methods to investigate the involvement of chromatin remodelers such as Srebp and Tip60, and the NSL complex in fibrosis-related processes including collagen synthesis and cell contraction. The article proposes the inhibition of Tip60 as a reliable therapeutic approach for treating cardiac fibrosis.

Overall, this paper demonstrates the integrity of its various components. Firstly, it provides a brief introduction to the impact of cardiac fibrosis on cardiac pathology and the fibroblast-associated transformation process. Subsequently, the article provides a detailed description of the specific methods employed, including bulk and single-cell CRISPR screening and epigenetic analysis. The authors then perform epigenetic analysis using the identified regulatory factors and smoothly present the strategy of Tip60 inhibition for treating cardiac fibrosis.

The strengths of the article are notable:

- 1. The article employs a comprehensive research design that combines bulk and single-cell CRISPR screening, providing more comprehensive information and deeper insights. It exhibits a high level of novelty.**
- 2. The study identifies several key regulatory factors, such as chromatin remodelers Srebp and Tip60, and the NSL complex, emphasizing their control over fibrotic states. These findings offer new perspectives and potential therapeutic targets for cardiac fibrosis.**
- 3. The researchers demonstrate how these chromatin factors enhance the activity of fibrosis-associated transcription factors during fibroblast transformation, revealing critical nodes and mechanisms within the regulatory network.**

We thank the reviewer for their comments and for suggesting aspects to improve our study. We appreciate the constructive feedback, including the need for further *in vivo* validation and the importance of adding human data to fully establish the therapeutic relevance of our findings. These are crucial points, and we agree that additional data will enhance the impact of our study. We are confident that these additional experiments and analyses address the reviewer's concerns and significantly strengthen the manuscript.

However, there are some limitations to the study:

- 1. The research primarily focuses on mouse cardiac fibroblasts, with relatively limited investigation of human cardiac fibroblasts. Further experiments in this area would be beneficial.**

We thank the reviewer for the valuable comment and fully agree that further investigation of human cardiac fibroblasts would significantly strengthen the translational relevance of our findings. To this point, we have performed additional analysis to address the relevance of our findings to human cardiac fibrosis and we have included the results in revised Fig. 6 and Extended Data Fig. 10.

First, we cross-referenced our *ex vivo* single-cell expression patterns with the single-cell expression patterns of human cardiac fibroblasts isolated from hearts in different clinical conditions^{1-3,6,7} (Fig. R26a). This analysis showed a clear correlation between our *ex vivo* murine fibroblast states and clinically relevant human cardiac subpopulations. For instance, our *ex vivo* naïve fibroblasts were related to human fibroblast subpopulations characteristic of healthy myocardium and our *ex vivo* myofibroblasts were related to fibrotic subpopulations of fibroblasts that appear in failure hearts from patients with myocardial infarction (MI) or Dilated (DCM), Hypertrophic (HCM) or Arrhythmogenic (ARVC) cardiomyopathies (Fig. R26b).

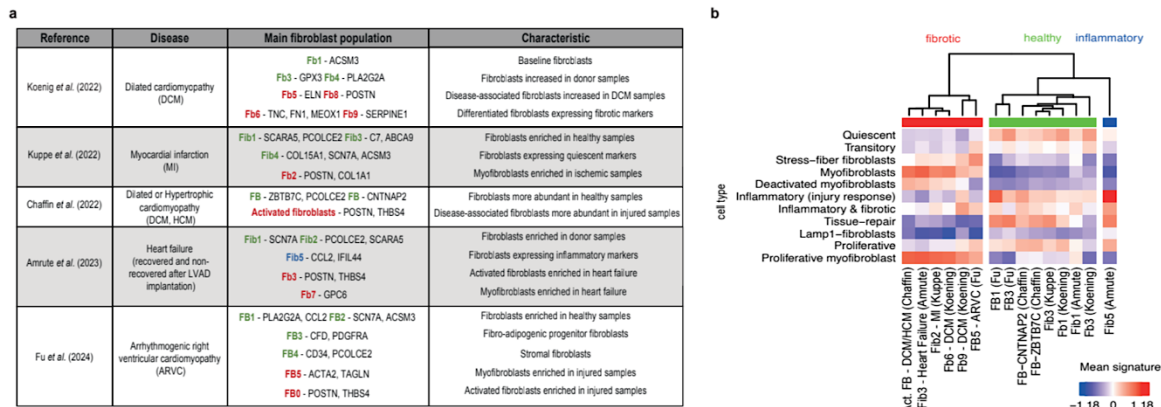


Figure R26 | *Ex vivo* single-cell expression patterns of murine cardiac fibroblasts are related to *in vivo* single-cell expression patterns of human cardiac fibroblasts. (a) Table summarizing key papers used for human signature comparisons conducted with the *ex vivo* murine data. (b) Enrichment of *in vivo* fibroblast expression signatures from references in (a) over *ex vivo* fibroblast populations from this study.

In addition, this analysis shows that depletion of some of our candidate targets (including *Kat5*, *Scrap* or *Wdr82*, and our positive control *Smad3*) in our *ex vivo* murine fibroblasts downregulated gene expression signatures specific of human fibrotic fibroblasts found in pathological conditions and, conversely, upregulated healthy fibroblast signatures (Fig. R27).

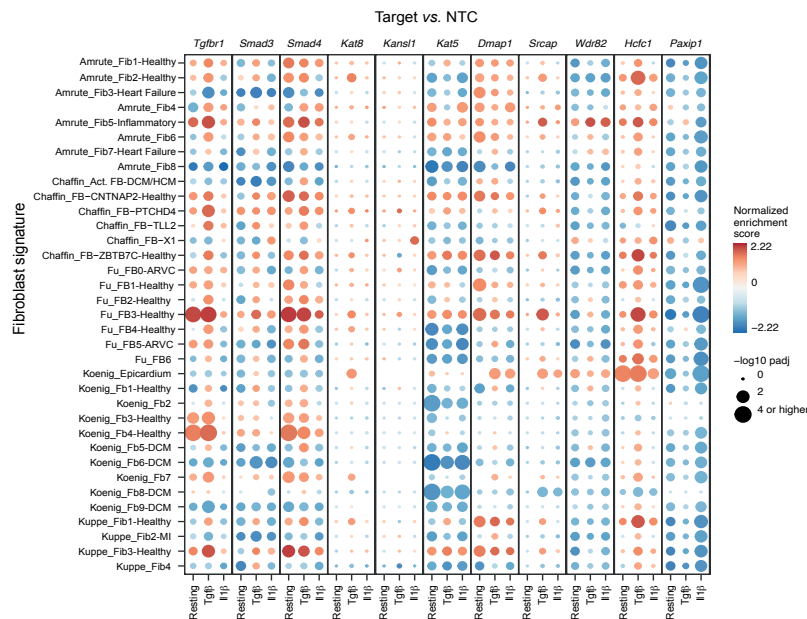


Figure R27 | Gene set enrichment analysis of differentially expressed genes across representative knockouts. Fibroblast expression signatures are taken from references in Fig. R26a. The color of each dot represents normalized enrichment score, the size represents the $-\log_{10}$ adjusted p-value.

Taken together, these results suggest a functional conservation (human-mouse) of the transcriptional regulators that orchestrate cardiac fibrotic responses. These results are part of the reviewed manuscript Fig.6a-b and Extended Data Fig. 10a.

Then, using RNA-seq, we analyzed the expression patterns of patient-derived cardiac fibroblasts pre-treated with vehicle or KAT5 inhibitor before TGF- β stimulation (Fig. R28a). TGF- β treatment induced a marked fibrotic response in unperturbed (vehicle) human cardiac fibroblasts characterized by the upregulation of typical hallmark fibrosis markers including POSTN, CTHRC1, ACTA2 (α -SMA) (Fig. R28b). Pre-treatment with KAT5 inhibitor reduced the fibrotic response to TGF- β , pushing cardiac

fibroblasts back to a healthy (unstimulated) state (Fig. R28b-d). Furthermore, patient-derived fibroblasts pre-treated with KAT5 inhibitor downregulated the transcriptional signatures characteristic of pathological human fibroblast subpopulations described above (Fib2-Kuppe, Fib6,8-9-Koenig, Act_FB-Chaffin, Fib3-Amrute, FB0-Fu) (Fig. R28e). These results were confirmed using genetic perturbation (CRISPR) of *KAT5* and qPCR measurements of four key fibrotic genes (Fig. R28f-g).

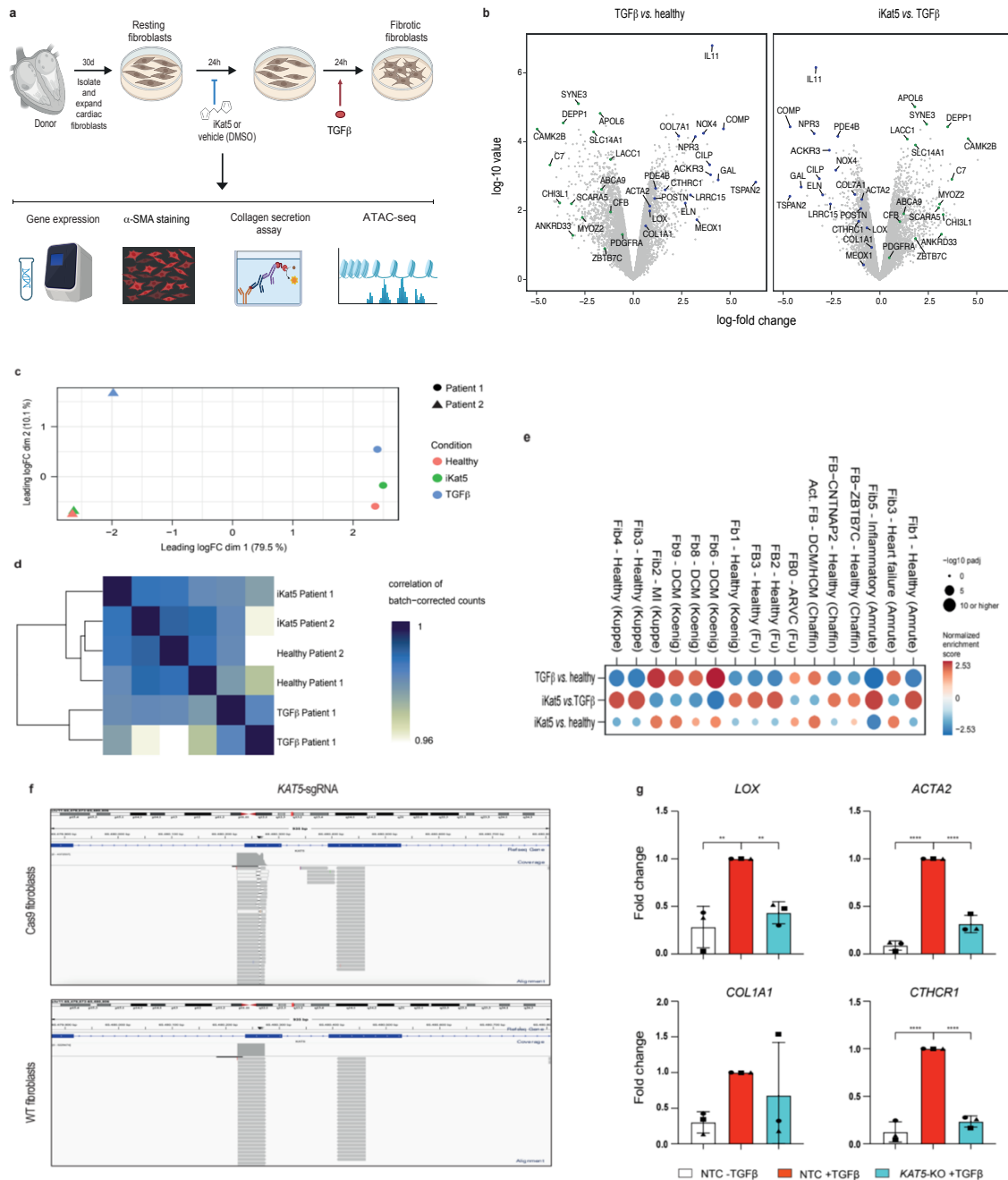


Figure R28 | KAT5 chemical and genetic perturbations attenuate fibrotic responses in human primary cardiac fibroblasts. (a) Schematic depiction of the experimental approach in human cardiac fibroblasts. (b) Differentially expressed markers of fibrosis in TGF-β-treated patient-derived cardiac fibroblasts (left) and in fibroblasts pre-treated with KAT5 inhibitor before the TGF-β stimulus (right). (c) Principal component analysis of gene expression in patient-derived cardiac fibroblasts. Dimension 1 corresponds to variability of gene expression between patients, while dimension 2 captures effects of TGF-β or KAT5 inhibitor on the transcriptome. (d) Correlation analysis of gene expression demarcates samples treated with TGF-β from unstimulated and KAT5-inhibited samples. (e) Gene set enrichment analysis of differentially expressed genes across treatments. Fibroblast expression signatures are taken from references in Fig. R26a. The color of each dot represents normalized enrichment score, the size represents the -log₁₀ adjusted p-value. (f) Genome browser snapshots of Indel-seq signal for *KAT5* loci in Cas9 and wildtype (WT) human cardiac fibroblasts transduced with *KAT5*-sgRNA. (g) Gene expression analysis (2^{-ΔΔCT}) of fibrotic markers in human cardiac fibroblasts depleted for KAT5 using CRISPR/Cas9 and then stimulated

with TGF- β . The measurements were performed in cell cultures from three different patients. Each patient is represented by a different symbol. Statistical significance was analyzed by one-way ANOVA test. ** $P < 0.01$, **** $P < 0.0001$. All data are mean \pm SD.

In addition, we measured stress-fiber formation and collagen deposition in patient-derived fibroblasts pre-treated with KAT5 inhibitor. These functional assays were conducted following 24 hours of TGF- β stimulation in control (vehicle) and NU-9056 (5 μ M) pre-treated human fibroblasts isolated from three different patients. The results show that KAT5 inhibition substantially reduces α -SMA protein levels and collagen secretion, providing direct evidence of its anti-fibrotic effects in human samples (Fig. R29a-b).

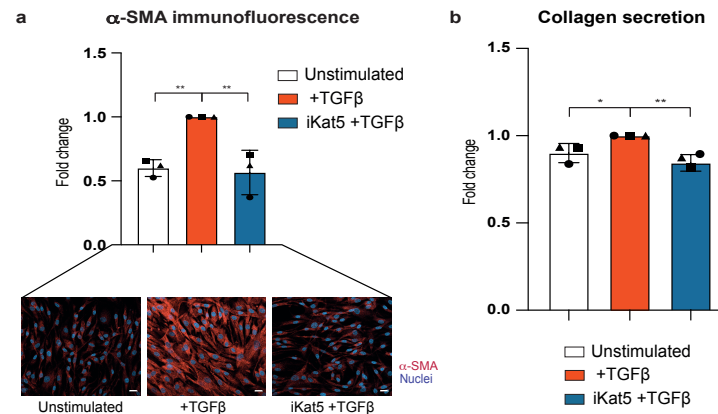


Figure R29 | KAT5 inhibition attenuates fibrotic responses in human primary cardiac fibroblasts. (a) Quantification of the average immunofluorescence intensity of α -SMA, following TGF- β stimulation in control and NU-9056 pre-treated human cardiac fibroblasts. The measurements were derived from three patients. Representative images of α -SMA immunostaining assays are shown at the bottom. Scale bars: 20 μ m. (b) Quantification of collagen secretion following TGF- β stimulation in control (vehicle) and NU-9056 pre-treated human cardiac fibroblasts. The measurements were performed in three patients. Each patient is represented by a different symbol. Statistical significance was analyzed by one-way ANOVA test. * $P < 0.05$, ** $P < 0.01$. All data are shown as fold change vs. TGF- β values and are mean \pm SD.

Finally, we analysed the chromatin accessibility patterns of patient-derived cardiac fibroblasts pre-treated with KAT5 inhibitor before TGF- β stimulation. This experiment showed a striking similarity with the murine results, where TEAD TF motifs showed a clear downregulation in their chromatin accessibility in human cardiac fibroblasts pre-treated with KAT5 inhibitor (Fig. R30). The strong similarity between human and mouse ChrF-TF dependencies suggests that the epigenetic mechanisms regulating fibrotic transformation in cardiac fibroblasts are conserved in mammals.

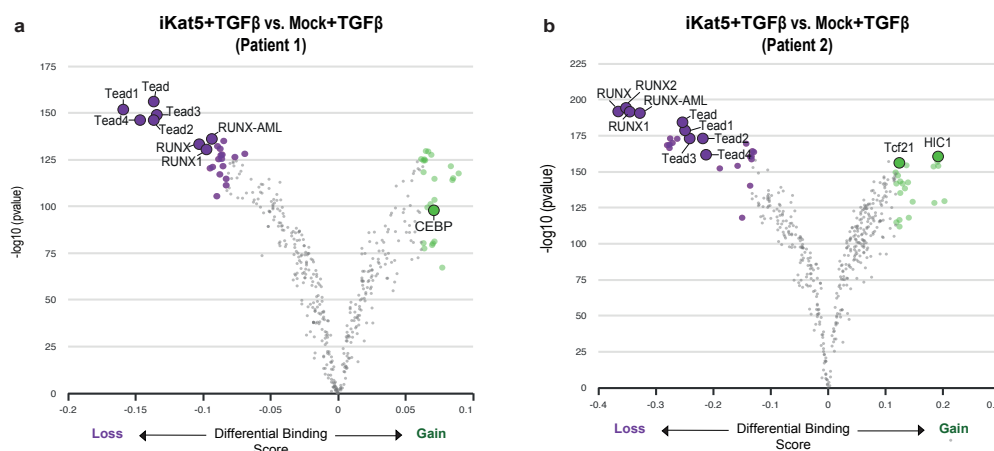


Figure R30 | Differential TF-footprinting analysis between control (vehicle) and NU-9056 pre-treated human fibroblasts after TGF- β stimulation. Dots in purple represent TF motifs with decreased accessibility in NU-9056 pre-treated human fibroblasts. Dots in green represent TF motifs with increased accessibility in NU-9056 pre-treated human fibroblasts. Patient 1 (a) and Patient 2 (b) are shown.

In conclusion, these results reinforce our findings suggesting KAT5 inhibition as a potential therapeutic avenue to alleviate cardiac fibrosis and have been included in revised Fig.6c-h and Extended Data Fig. 10c-g.

2. The article lacks extensive *in vivo* animal experiments, with most of the content centered around *ex vivo* fibroblasts. Including more *in vivo* experiments would be valuable.

We agree with the reviewer that *in vivo* evaluation of Kat5 inhibition is crucial to better understand its therapeutic potential for treating fibrotic diseases.

To address this, we have initiated experiments using a murine model of myocardial infarction (MI). Adult mice (10 weeks old) were subjected to permanent ligation of the left descending coronary artery as previously described by our group⁸, and groups of 7-9 mice were treated with either NU-9056 Kat5 inhibitor (10 mg/kg) or DMSO vehicle as a control starting 3 days post-MI and continued daily for 21 days. Cardiac function was assessed by echocardiography (Vevo 3100 imaging system) at day 2 and day 30 post-infarction (Fig. R31a). NU-9056-treated mice demonstrated improved cardiac remodeling, with stable diastolic and systolic volumes and areas one month post-MI, unlike the vehicle-treated controls, which showed significant heart dilation (Fig. R31b).

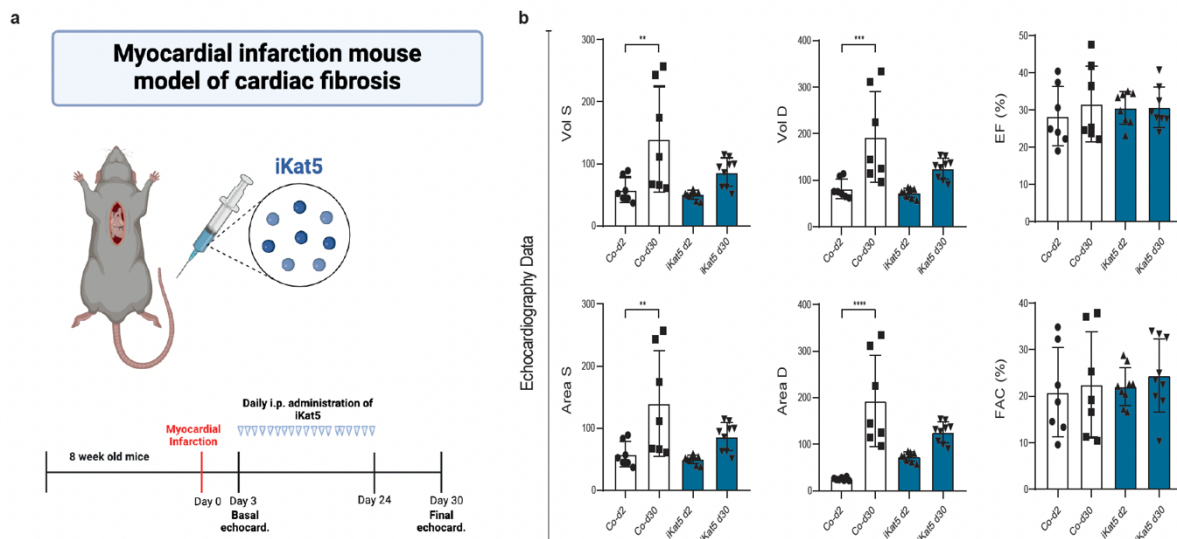


Figure R31 | Administration of Kat5 chemical inhibitor NU-9056 preserves cardiac deleterious remodeling after MI. (a) Schematic depiction. Echocardiography studies were performed at day 2 (basal) and day 30 (final) post-MI in mice daily treated with NU-9056 (10 mg/kg) (or vehicle), beginning on day 3 after MI, for 21 consecutive days. **(b)** Echocardiography data. Cardiac systolic (S) and diastolic (D) ventricle areas (mm²) and volumes (μL), ejection fraction (EF) (%) and fractional area change (FAC) (%) were measured. Statistical significance was calculated by ANOVA with multiple comparisons test between day 2 and day 30 post-MI and is represented as **P < 0.01, ***P < 0.001, and ****P < 0.0001. Data were obtained from 7-9 animals per group. Mean ± SD values are represented.

These results are promising but we have noticed that demonstrating the beneficial effects of Kat5 inhibition *in vivo* requires further optimization of Kat5 inhibitor delivery and a deep characterization of fibroblast dynamics during myocardial healing in infarcted animals. This represents a significant extension of the work presented in this paper. Given that we have already expanded significantly the study by incorporating: a) analysis of fibrotic responses in fibroblasts isolated from 3 other organs and b) a deep analysis of KAT5 inhibition in patient-derived fibroblasts, we feel that these *in vivo* studies fall beyond the scope of the current article.

It is worth noting that a different Kat5 inhibitor, TH1834, has been described in the literature⁹ and shown to be effective in a murine model of MI, improving systolic function and reducing cardiac apoptosis and fibrosis.

Nevertheless, even in its current form, this article remains highly valuable and relevant to a broad audience.

We highly appreciate this positive feedback.

References:

1. Chaffin, M. *et al.* Single-nucleus profiling of human dilated and hypertrophic cardiomyopathy. *Nat.* 2022 6087921 **608**, 174–180 (2022).
2. Koenig, A. L. *et al.* Single-cell transcriptomics reveals cell-type-specific diversification in human heart failure. *Nat. Cardiovasc. Res.* 2022 13 **1**, 263–280 (2022).
3. Amrute, J. M. *et al.* Defining cardiac functional recovery in end-stage heart failure at single-cell resolution. *Nat. Cardiovasc. Res.* **2**, 399–416 (2023).
4. Khalil, H. *et al.* Fibroblast-specific TGF- β -Smad2/3 signaling underlies cardiac fibrosis. *J. Clin. Invest.* **127**, 3770–3783 (2017).
5. Nagaraju, C. K. *et al.* Myofibroblast Phenotype and Reversibility of Fibrosis in Patients With End-Stage Heart Failure. *J. Am. Coll. Cardiol.* **73**, 2267–2282 (2019).
6. Kuppe, C. *et al.* Spatial multi-omic map of human myocardial infarction. *Nat.* 2022 6087924 **608**, 766–777 (2022).
7. Fu, M. *et al.* Single-cell RNA sequencing in donor and end-stage heart failure patients identifies NLRP3 as a therapeutic target for arrhythmogenic right ventricular cardiomyopathy. *BMC Med.* **22**, (2024).
8. Ruiz-Villalba, A. *et al.* Single-Cell RNA Sequencing Analysis Reveals a Crucial Role for CTHRC1 (Collagen Triple Helix Repeat Containing 1) Cardiac Fibroblasts After Myocardial Infarction. *Circulation* **142**, 1831–1847 (2020).
9. Wang, X. *et al.* Pharmacological inhibition of the acetyltransferase Tip60 mitigates myocardial infarction injury. *Dis. Model. Mech.* **16**, (2023).

REVIEWER COMMENTS

Reviewer #1 (Remarks to the Author):

R1Q1 and R1Q6 - Statistical analyses should be performed for the new human data (flow data on PDGFR α and IF data on H2AZac), and point out when comparisons are not significant.

We appreciate the reviewer's comment. We would like to clarify that statistical analyses were performed for both new human data and despite a clear tendency was found, not statistical significance was reached. We have now added this sentence "Statistical significance was analyzed by *xx* test and is indicated as follows: **P* <0.05, ***P* <0.01, ****P* <0.001, *****P* <0.0001" in all figure captions of the manuscript in which a statistical test has been performed to help understand how statistical significance is represented.

To further strengthen the results, flow cytometry analysis of PDGFR α expression in human cardiac fibroblasts from a fourth patient was performed. Again, these fibroblasts were cultured under three conditions: unstimulated, stimulated with TGF- β , and pre-treated with the KAT5 inhibitor (NU-9056) before TGF- β stimulation. Consistent with the results from the other three patients, this fourth patient's fibroblasts showed moderate PDGFR α expression in the unstimulated condition, a downregulation of PDGFR α upon TGF- β stimulation, and a restoration of PDGFR α expression with pre-treatment using the NU-9056 inhibitor. Notably, with the inclusion of this fourth patient, statistically significant differences in PDGFR α expression were observed between Unstimulated vs. +TGF β and iKAT5+TGF β vs. +TGF β conditions (**Fig. R1Q1**).

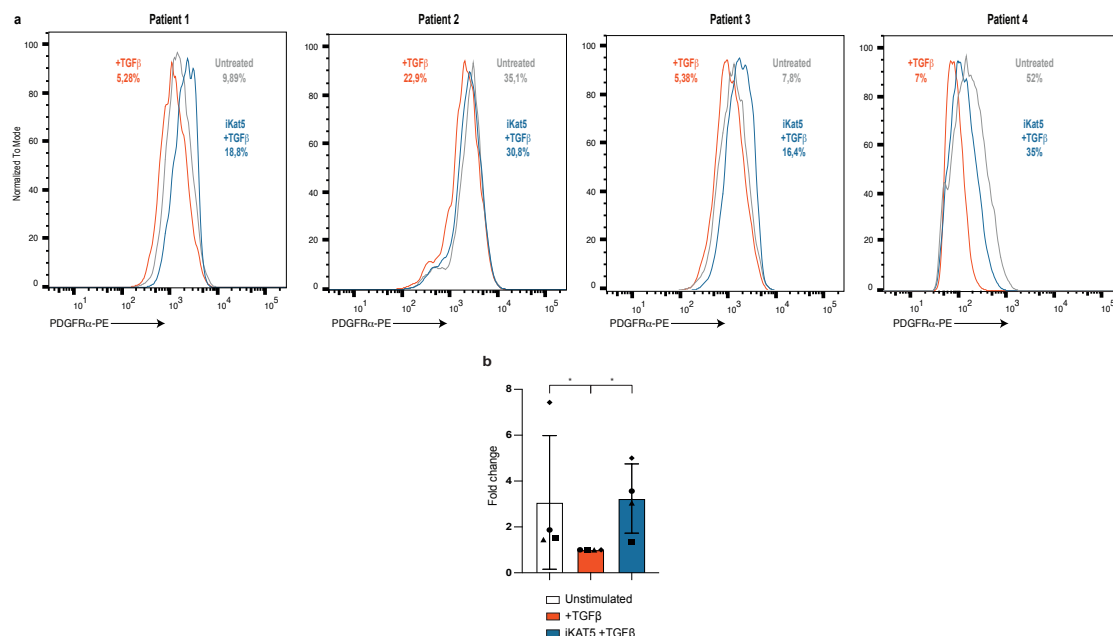


Figure R1Q1 | PDGFR α expression in human cardiac fibroblasts. (a) FACS analysis for PDGFR α in human cardiac fibroblasts (obtained from four different patients undergoing cardiac surgery) in unstimulated (grey), TGF- β stimulated (red) and NU-9056 (5 μ M) pre-treated (blue) cells. (b) Quantification of the percentage of PDGFR α positive cells, following TGF- β stimulation in control and NU-9056 pre-treated human cardiac fibroblasts. The measurements were derived from four patients who underwent cardiac surgery. Each patient is represented by a different symbol. All data are shown as fold change vs. TGF- β values and are mean \pm SD. Statistical significance was analyzed by Kruskal-Wallis test and is indicated as follows: **P* <0.05.

Similarly, H2AZac levels were analyzed by immunofluorescence in human cardiac fibroblasts cultured under the same three conditions. Despite including a fourth patient, statistical significance was not reached. However, a decreasing trend was observed between the iKAT5+TGF β vs. +TGF β conditions ($p = 0.088$), suggesting the potential inhibitory effect of NU-9056 on H2AZac (Fig. R1Q6). This lack of statistical significance is likely due to inter-patient variability, which is expected given the heterogeneous nature of samples from different individuals.

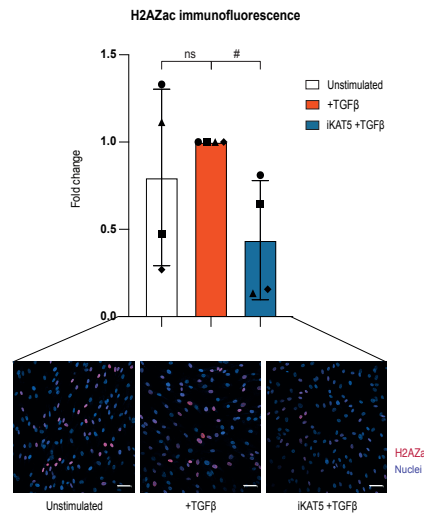


Figure R1Q6 | Kat5 inhibition attenuates H2AZ acetylation levels in human primary cardiac fibroblasts. Quantification of the percentage of H2AZac positive cells, following TGF- β stimulation in control and NU-9056 pre-treated human cardiac fibroblasts. The measurements were derived from four patients who underwent cardiac surgery. Each patient is represented by a different symbol. Representative images of H2AZac immunostaining assays are shown at the bottom. Scale bars: 50 μ m. All data are shown as fold change vs. TGF- β values and are mean \pm SD. Statistical significance was analyzed by one-way ANOVA test. No significant difference in H2AZac levels was observed between the untreated and TGF- β treated conditions. However, a decreasing trend was noted between the iKAT5+TGF β vs. +TGF β conditions ($p = 0.088$).

R1Q8 - Second half of the response does not adequately address original concern. It would be helpful to include unstimulated control to Extended Data Fig. 8k because it would show if the reversion goes back down to baseline.

We appreciate the reviewer's suggestion to include unstimulated controls in Extended Data Fig. 8k. In response, we have conducted three additional experiments with an unstimulated control condition, and the results have been now incorporated into the updated Extended Data Fig. 8k. The addition of the unstimulated control highlights how the gene expression levels of key fibrotic genes return to near-baseline levels in activated fibroblasts treated with the Kat5 inhibitor (Fig. R1Q8).

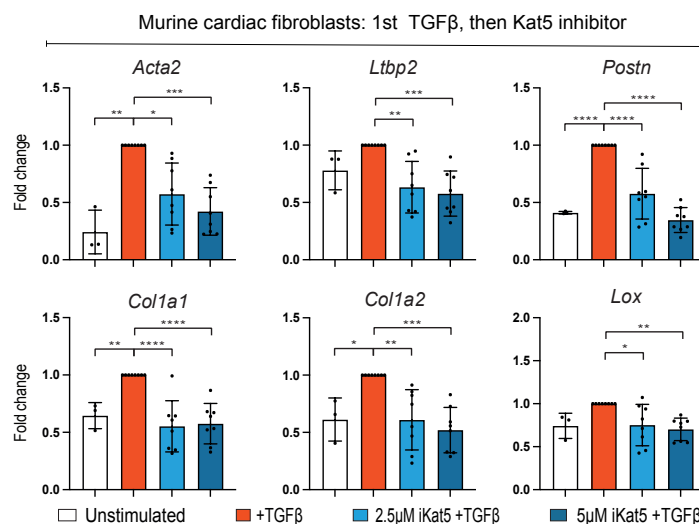


Figure R1Q8 | Kat5 inhibition attenuates fibrotic responses in murine cardiac fibroblasts. Relative expression ($2^{-\Delta\Delta CT}$) of fibrotic marker genes in unstimulated control (vehicle) or following TGF- β stimulation in control (vehicle) and NU-9056 treated murine cardiac fibroblasts. The measurements were performed in three-eight replicate experiments. All data are shown as fold change vs. TGF- β values and are mean \pm SD. Statistical significance was analyzed using one-way ANOVA or Kruskal-Wallis tests and is indicated as follows: * $P < 0.05$, ** $P < 0.01$, *** $P < 0.001$, **** $P < 0.0001$.

R1Q10 – It is disappointing that FAP could not be observed in the scRNA-seq after TGFb and IL-1B treatment. This finding raises issues as to whether TGFb and IL-1B treatment in vitro is actually able to activate fibroblasts, which is a key point of the authors studies.

We understand the reviewer's concern about FAP expression in activated cardiac fibroblasts after TGF β and IL1 β treatments *ex vivo*. In scRNA-seq data (Perturb-seq of cells harbouring non-targeting guides), we find an up-regulation of FAP in the TGF β -treated condition, suggesting that fibroblasts become activated upon TGF β treatment (**Fig. R1Q10a**). However, FAP was lowly expressed overall and was thus filtered out by bioinformatics pre-processing pipelines. Confirming this issue, when checking FAP expression in cardiac fibroblasts in the scRNA-seq database CELLxGENE (<https://cellxgene.cziscience.com/>), we also found low FAP expression, for example in the Tabula Muris scRNA-seq atlas. In consequence, as it appears difficult to quantify FAP in sufficient depth using scRNA-seq, we prefer to not further comment on FAP expression in the manuscript. Nevertheless, our data show a trend in the direction expected by this reviewer and our protein data (checked by immunofluorescence of FAP in cardiac fibroblasts cultured under the three conditions: unstimulated, TGF β - and IL1 β -stimulated) also confirm the expected FAP upregulation in TGF β -treated cells (**Fig. R1Q10b**), validating our model system.

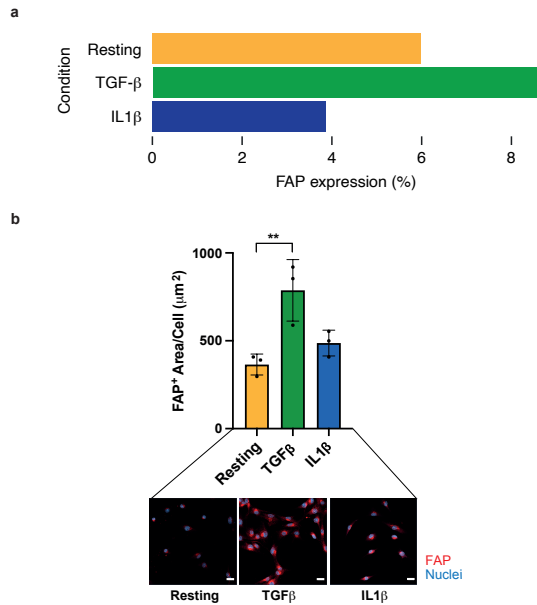


Figure R1Q10 | FAP expression in murine cardiac fibroblasts. **a)** Percentage of cells with detectable FAP expression (at least one FAP read detected) in our Perturb-seq data, separated by condition. In most cells, only 1-2 reads per cell were detected. **b)** Quantification of FAP⁺ expression in unstimulated, TGF β - and IL1 β -stimulated cells analyzed by immunofluorescence. The measurements were performed in three replicate experiments. Representative images of FAP immunostaining assays are shown at the bottom. Scale bars: 20 μm . All data are mean \pm SD. Statistical significance was analyzed by one-way ANOVA test and is indicated as follows: ** $P < 0.01$.

R2Q1 - The authors mention that Kat5 inhibition has already been shown to help with fibrosis after MI with TH1834 (PMID: 36341679). The authors should show how their drug (NU-9056) compares to an already established drug, at least in their *in vitro* assays, to put their results in context with previously published results.

We appreciate the reviewer's comment. To compare both Kat5 inhibitors, we performed additional *in vitro* assays using murine cardiac fibroblasts cultured under four conditions: unstimulated, stimulated with TGF- β , and pre-treated with either NU-9056 or TH1834 prior to TGF- β stimulation.

The results demonstrate that both inhibitors have similar effects, reducing fibrotic gene expression, decreasing α -SMA protein levels, and lowering collagen secretion (**Fig. R2Q1**). These findings suggest that NU-9056 exerts comparable anti-fibrotic effects to TH1834, further supporting the role of Kat5 in modulating fibroblast activation.

This validation with another Kat5 inhibitor is now mentioned in the discussion section of the manuscript (page 8, lines 386-388) to contextualize our results within the framework of previously published data and strengthen our findings with the NU-9056 inhibitor.

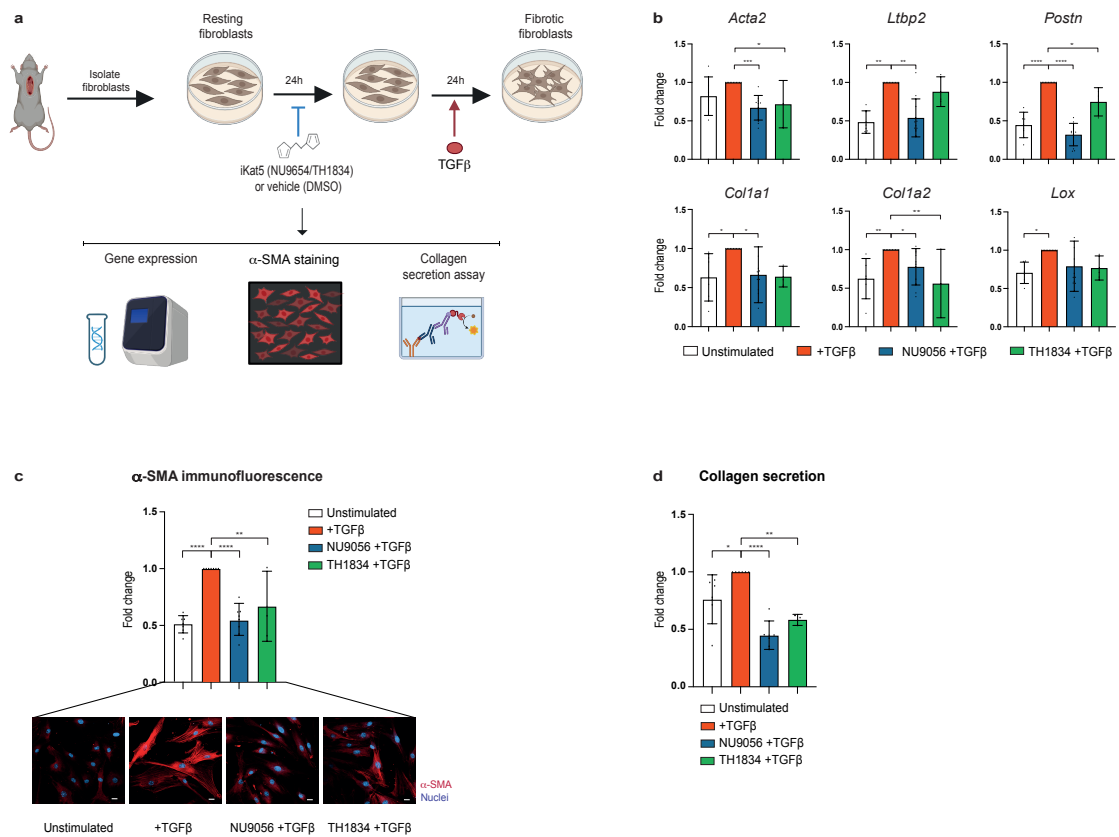


Figure R2Q1 | Kat5 inhibition attenuates fibrotic responses in murine cardiac fibroblasts. (a) Schematic depiction of the experimental approach in murine cardiac fibroblasts. (b) Expression of fibrotic marker genes following TGF- β stimulation in control, NU-9056 and TH1834 pre-treated murine cardiac fibroblasts. The measurements were performed in three-eleven replicate experiments. (c) Quantification of the average immunofluorescence intensity of α -SMA, following TGF- β stimulation in control, NU-9056 and TH1834 pre-treated murine cardiac fibroblasts. The measurements were performed in three-seven replicate experiments. Representative images of α -SMA immunostaining assays are shown at the bottom. Scale bars: 20 μ m. (d) Quantification of collagen secretion following TGF- β stimulation in control, NU-9056 and TH1834 pre-treated murine cardiac fibroblasts. The measurements were performed in three-six replicate experiments. All data are shown as fold change vs. TGF- β values and are mean \pm SD. Statistical significance was analyzed by one-way ANOVA or Kruskal-Wallis tests and is indicated as follows: * P < 0.05, ** P < 0.01, *** P < 0.001, **** P < 0.0001.

REVIEWER COMMENTS

Reviewer #4

In this revised manuscript from Aguado-Alvaro et. al. Authors sufficiently satisfied the major comments. It is of note however the level of fibroblast activation of naive cardiac fibroblast in humans. As previously noted fibroblast in post infarction state can acquire a steady state phenotype and may already have an elevated fibrotic state and thus TGF- β stimulation may not make a bigger difference. This point would be important to add to the discussion section and address that the study did not have naive human fibroblasts to assess. Nonetheless the revision is sufficient for acceptance.

We thank the reviewer for the positive evaluation. As recommended, we now mention in the Discussion section that the human fibroblasts used in this study may exhibit a fibrotic state activated due to their origin (lines 380-385).

Reviewer #5

1. The authors should provide more information regarding the region of the “discarded” tissue. Is it atrial appendage? Were any quality control measures performed on the human fibroblasts regarding their purity and activation state?

Human cardiac fibroblasts used in this study were primary cell cultures isolated from discarded atrial appendage obtained from patients during surgical cardiac interventions.

Human cardiac fibroblasts were isolated through low mechanical tissue enzymatic digestion using collagenases, followed by explant outgrowth, as applied in previous studies from the group^{1,2}. After isolation, the expression of fibroblast-related genes (such as *COL1A1*, *FNI*, and *LOX*) and the ability of the cells to respond to TGF- β were routinely assessed. Functional responsiveness to TGF- β , evidenced by upregulation of the myofibroblast marker *ACTA2* and increased expression of collagen (*COL1A1*) and collagen-processing enzymes (e.g., *LOX*), was confirmed. Only cultures that demonstrated robust expression of fibroblast markers and a clear response to TGF- β were included in downstream experiments. Additionally, the fibroblasts initially exhibited the typical spindle-shaped morphology, which transitioned to a myofibroblast-like phenotype with prominent stress fiber formation following TGF- β stimulation.

This information has now been updated into the Methods section of the revised manuscript (lines 460 and 477-480).

2. Isotype matched controls should be used for flow cytometry. Not unstained cells. What were the controls for the α SMA intracellular staining?

As suggested, we have included isotype controls for PDGFR α staining in mouse and human cardiac fibroblasts, confirming staining specificity (**Figure R5Q2a**).

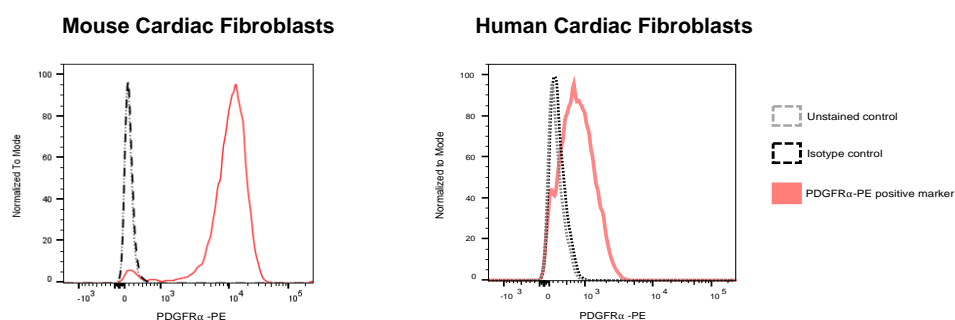


Figure R5Q2a | Histogram showing unstained (grey), isotype (black) controls, and positive staining (red) for mouse PDGFR α antibody (#553930, BD Pharmingen) and human PDGFR α antibody (#130-115-238, Miltenyi). Unstained and IgG isotype controls used at the same concentration as the anti-PDGFR α antibodies, confirm minimal nonspecific signal and validate the specificity of PDGFR α staining.

For α -SMA-Cy3 staining, an isotype control was not used due to the lack of commercially available Cy3-conjugated isotype antibodies. Instead, we employed permeabilized unstained cells as negative controls to establish background fluorescence levels and define appropriate gating strategies for intracellular α -SMA staining.

The specificity of α -SMA antibody as well as the key antibody PDGFR α is also supported by their expected staining patterns (using consistent antibody dilutions and settings) after TGF- β treatment, showing a clear shift between unstimulated and stimulated states, especially in serum-free media (**Figure R5Q2b**). Any nonspecific binding would uniformly affect all samples and not alter the qualitative conclusions.

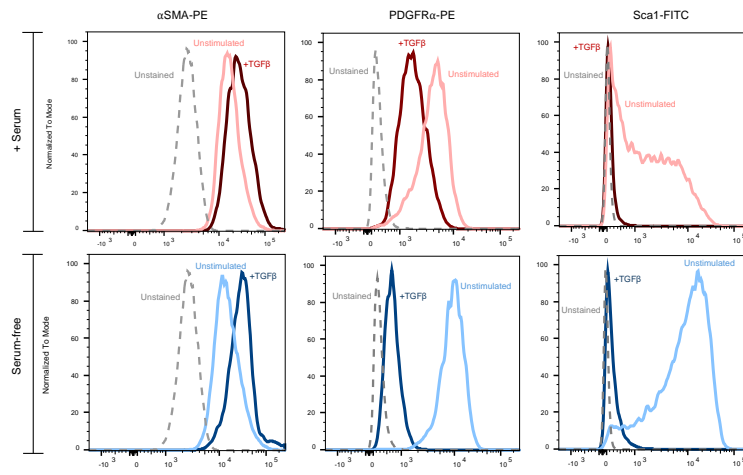


Figure R5Q2b | Representative FACS analysis of intracellular alpha smooth actin (α -SMA), PDGFR α and Sca-1 in unstimulated and TGF- β stimulated fibroblasts grown under serum-free (blue) and serum-containing (red) conditions. These histograms include unstained controls (in grey) to define background signal and support gating decisions.

Additionally, we clarify that all flow cytometry antibodies used in this study included unstained controls to establish background fluorescence and gating strategies, as shown in Figures **R5Q2a–d**, displaying well-separated signals for positive markers.

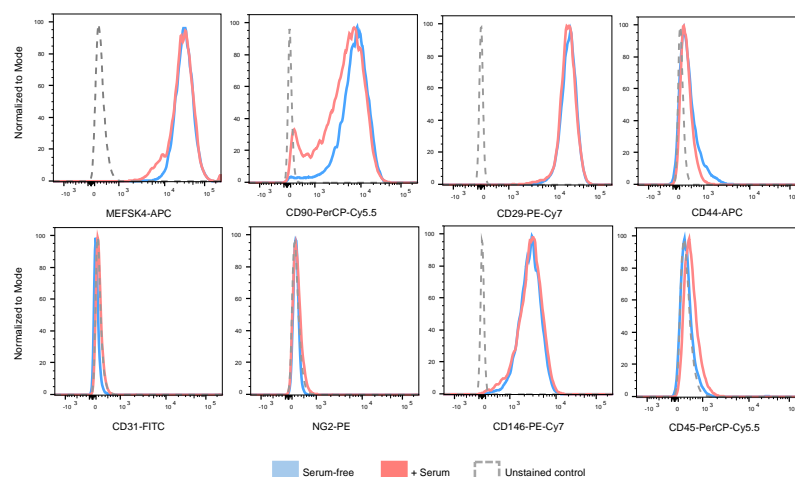


Figure R5Q2c | Representative FACS analysis of fibroblast-stromal (MEFSK4, CD90, CD44, CD29), pericytes (CD146, NG2), endothelial (CD31) and hematopoietic (CD45) cell markers in fibroblasts grown under serum-free (blue) and serum-containing (red) conditions at day 4 of culture. Histograms also include unstained control cells (grey) to define background fluorescence and aid in gating.

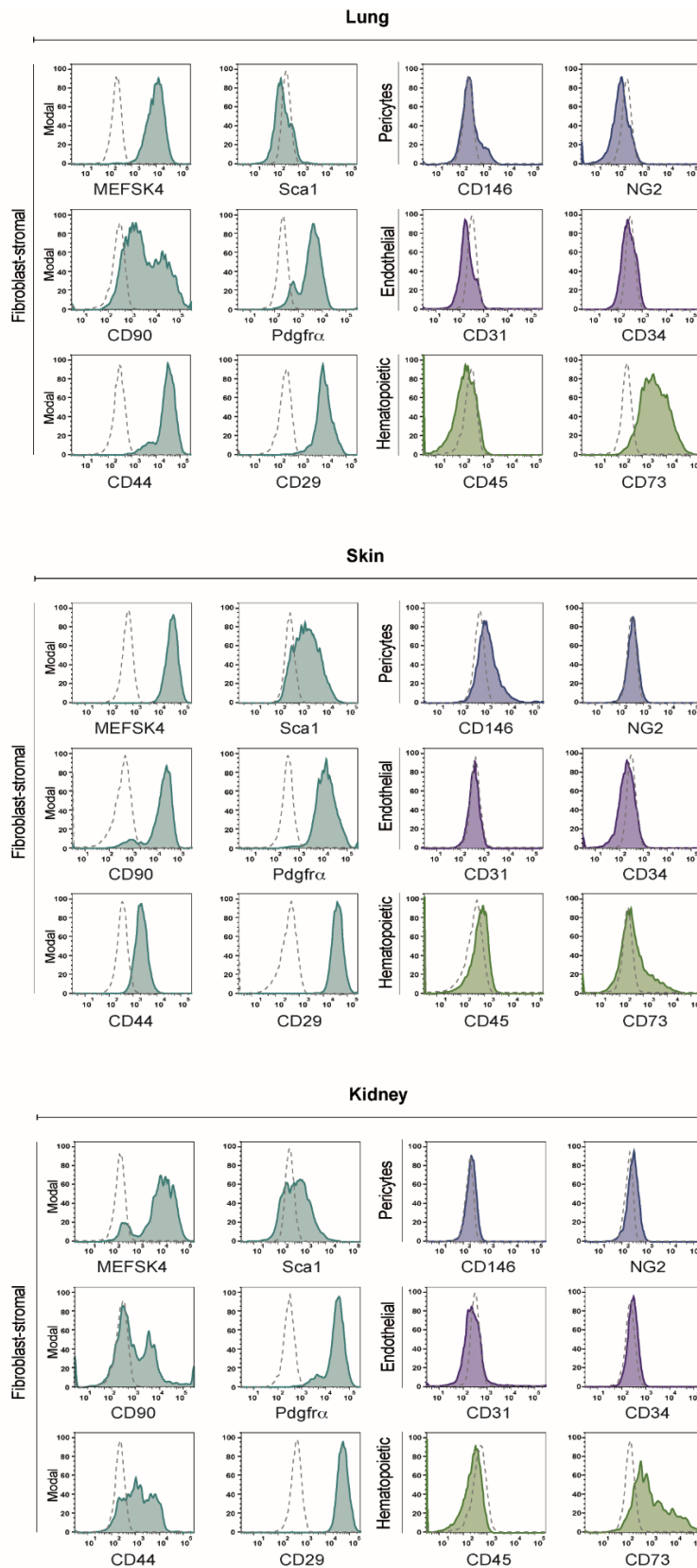


Figure R5Q2d | Characterization of lung, skin, and kidney fibroblasts through flow cytometry. Representative FACS analysis of fibroblast-stromal (MEFSK4, CD90, CD73, CD44, CD29), pericyte (CD146, NG2), endothelial (CD31, CD34), and hematopoietic (CD45) markers in unstimulated lung, skin, and kidney fibroblasts at day 7 of culture. Histograms also include unstained control cells (grey) to define background fluorescence and aid in gating.

The high specificity of the antibodies is further supported by supplier documentation, including representative histograms comparing isotype controls with specific staining (**R5Q2e**).

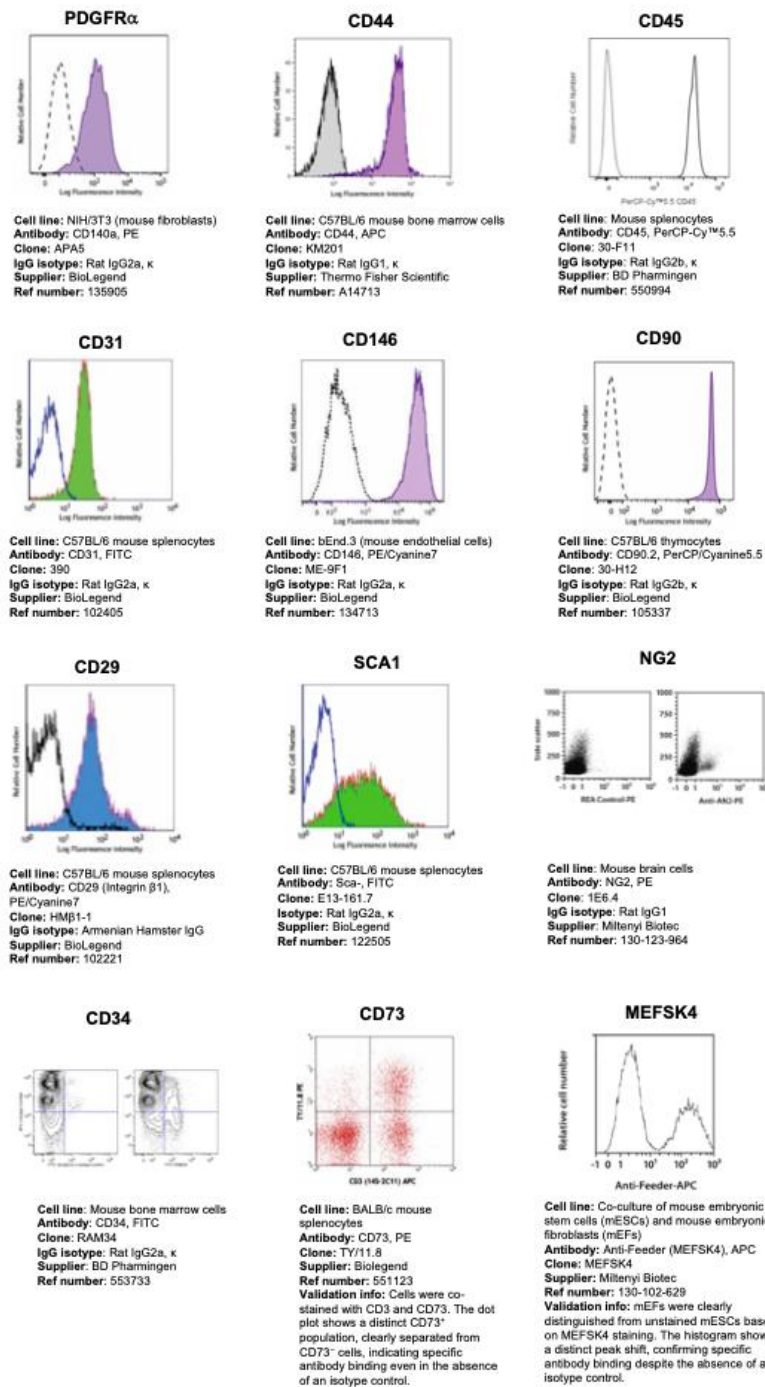


Figure R5Q2e | Histograms from commercial suppliers display antibody staining alongside their respective isotype controls. The cell line used for testing, along with details such as the antibody and fluorochrome, clone, isotype specificity, supplier, and reference number, are indicated.

Together, these multiple lines of evidence, including negative controls, manufacturer specificity data, experimental-responsive signal shifts, and isotype validation for PDGFR α marker, support the specificity and reliability of our flow cytometry data.

3. Authors should specify which TGF β was used in the experiments. Providing catalog numbers throughout the m&m would provide transparency. Also, the term unstimulated fibroblasts is a bit misleading as the culture conditions have bFGF. The culture conditions for the fibroblasts is unclear. In the text the authors mention serum free conditions, but for the human fibroblast 10% FBS is listed. The statement that the serum free conditions maintain a rested state is not thoroughly substantiated based on the data shown in extended figure 1. The data seem to suggest that the cells might be more responsive to TGF β stimulation.

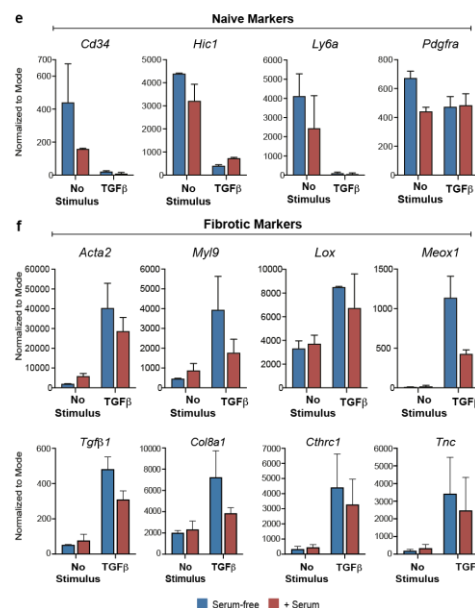
The catalog number for the TGF- β used (PeproTech #100-21), along with the catalog numbers for all relevant reagents, has been added throughout the Methods section.

In our study, “unstimulated” specifically refers to the absence of TGF- β (a potent pro-fibrotic factor) and IL-1 β (an inflammatory cytokine). While bFGF is present in all experimental conditions to support cell maintenance, it exerts only minimal activating effects *in vitro*. The addition of TGF- β or IL-1 β induces robust pro-fibrotic or inflammatory responses, respectively, highlighting their central role in fibroblast activation in our model.

We also acknowledge the need to clarify the culture conditions used across species. Murine cardiac fibroblasts were cultured in a defined, serum-free medium to minimize baseline activation, while human cardiac fibroblasts were maintained in 10% FBS-containing medium, as per protocols optimized by clinical collaborators^{1,2}. The latter reflects the partial pre-activation status of patient-derived cells and their higher dependency on serum for viability and proliferation.

For murine cells, KnockOut Serum Replacement (KSR) was used instead of fetal bovine serum (FBS) to minimize background TGF- β exposure and better maintain fibroblast quiescence. KSR provides a chemically defined medium that preserves cell viability without promoting fibroblast activation. This strategy enhances the distinction between basal and activated states, as shown by transcriptomic analyses: fibroblasts cultured in serum-free conditions exhibit elevated expression of naïve-associated markers and reduced expression of fibrotic markers in the absence of stimulation (**Manuscript Extended Data Fig. 1e–f**). Therefore, serum-free culture effectively maintains a more quiescent fibroblast phenotype, facilitating more accurate assessment of responses to pro-fibrotic or inflammatory cues.

Extended Data Fig. 1



Extended Figure 1 | Characterization of the fibroblast *ex vivo* screen system. (e-f) Expression levels of naïve (e) and fibrotic (f) markers in serum-free (blue) and serum-containing (red) conditions. Values are normalized read counts from two independent experiments. Data are mean \pm SD.

4. The authors need to clarify if the data in figures represents separate isolations, replicate wells, or different passages of fibroblasts.

We clarified in the figure legends, Methods section, and Reporting Summary whether the data refer to independent cell isolations or replicate wells.

5. Regarding the PDGFR α expression in human fibroblasts, an essential control is missing from the flow data. That is treatment with iKAT5 alone. Data should not be presented as fold change in percentage as it appears all cells still remain positive for PDGFR α . It seems that there is an increase in mean fluorescence intensity. For reference, the authors should include a negative control.

Western blotting for protein amount, might also shed some light on whether the receptor is endocytosed and still present or if there is a loss of protein.

As suggested, we have included an iKAT5-only treatment condition and a negative control to assess the inhibitor's isolated effect and background fluorescence, respectively (**Figure R5Q5a**). We reanalyzed the data using MFI-based quantification of surface PDGFR α (**Figure R5Q5b**), revealing a significant increase in expression upon KAT5 inhibition in TGF- β -stimulated cells, and a trend toward increased expression in unstimulated cells, suggesting partial reversal of a pre-activated fibroblast state.

While we acknowledge the value of Western blotting to assess receptor internalization, we consider this beyond the scope of the current study, which focuses on surface PDGFR α as a marker of fibroblast activation.

We believe that our current data, including FACS analysis with MFI quantification and appropriate controls, are sufficient to support our conclusions regarding surface receptor expression and activation state of human cardiac fibroblasts.

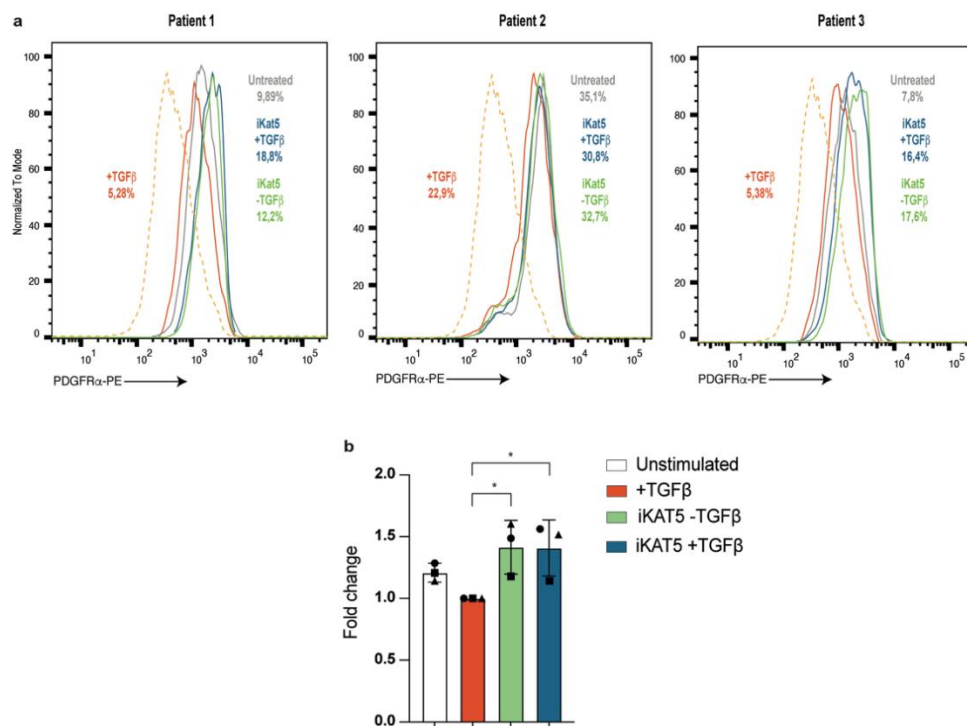


Figure R5Q5 | PDGFR α expression in human cardiac fibroblasts. (a) FACS analysis for PDGFR α in human cardiac fibroblasts (obtained from three different patients undergoing cardiac surgery). Cells were cultured under the following conditions: unstimulated (grey), TGF- β stimulated (red), pre-treated with the KAT5 inhibitor NU-9056 before TGF- β stimulation (blue), and treated with NU-9056 alone (green). Negative controls are shown in orange for reference. (b) Quantification of mean fluorescence intensity (MFI) for each condition. The measurements were derived from three patients who underwent cardiac surgery. Each patient is represented by a different symbol. All data are shown as fold change vs. TGF- β

values and are mean \pm SD. Statistical significance was analyzed by one-way ANOVA test and is indicated as follows: *P < 0.05.

6. Does the observed reduction in PDGFR α affect the signaling of this pathway?

Assessing the impact of PDGFR α modulation on downstream PDGF signaling would offer valuable mechanistic insight; however, this lies beyond the scope of the current study. In our work, PDGFR α is primarily used as a phenotypic marker to distinguish naïve vs. fibrotic fibroblast states, rather than as a readout of PDGF signaling activity. Investigating functional consequences would require additional analyses, such as ligand stimulation and downstream effector assessment.

7. Data for F R1Q10 should be presented as % of positive cells. Not FAP area/cell. The “resting” cells do not appear to be spread on the plate. Analyses should be performed when cells have attached for the same period of time.

We appreciate the reviewer’s concern regarding potential misquantification of FAP due to uneven cell distribution or adhesion time. However, all experiments were performed under consistent conditions, with equal seeding densities and adhesion times across groups. The observed morphological differences, such as the more elongated and spread-out appearance of TGF- β -treated cells vs. the compact morphology of resting cells, are characteristic of fibroblast activation and not indicative of attachment discrepancies.

To further control for area-related variability, we reanalyzed FAP expression normalized to cytoskeletal area using dual immunofluorescence for FAP and phalloidin (**Figure R5Q7**). This approach confirms significant FAP upregulation in TGF- β -treated cells and supports our conclusion that TGF- β induces fibroblast activation.

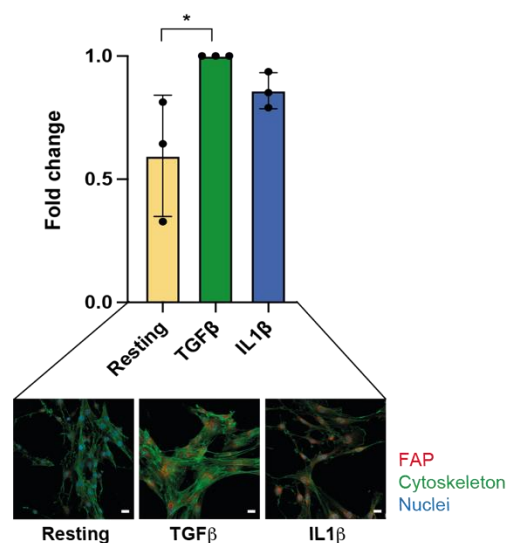


Figure R5Q7 | FAP expression in murine cardiac fibroblasts. Quantification of FAP expression in unstimulated, TGF β - and IL1 β -stimulated cells analyzed by immunofluorescence. The measurements were performed in three independent experiments. Representative images of FAP/Phalloidin immunostaining assays are shown at the bottom. Scale bars: 20 μ m. All data are shown as fold change vs. TGF- β values and are mean \pm SD. Statistical significance was analyzed by one-way ANOVA test and is indicated as follows: *P < 0.05.

8. Images in panel C of R2Q1 suggest that all cells are alpha smooth muscle actin positive. Again, Western blotting would provide a better understanding of the amount of aSMA than ICC. The number of replicates for the TH1834 +TGFβ treatment is not readily apparent.

In our study, α -SMA expression was consistently assessed by immunofluorescence across all experimental models (mouse, human, and organ-level), a widely accepted method in the field^{3,4}. As shown in **Figure R2Q1c**, cardiac fibroblasts exhibit basal α -SMA levels under unstimulated conditions, with a marked increase upon TGF- β stimulation, indicated by enhanced red fluorescence. Quantification was performed using ImageJ by measuring background-corrected fluorescence intensity per cell, ensuring objective and reproducible results. These findings align with our gene expression data from Perturb-seq, qPCR, and human RNA-seq (Manuscript Figures 3a, 4g, 5b–d, 6d).

The TH1834 + TGF- β condition was tested in three independent replicate experiments. To enhance clarity, data point size was increased in **Fig. R5Q8**.

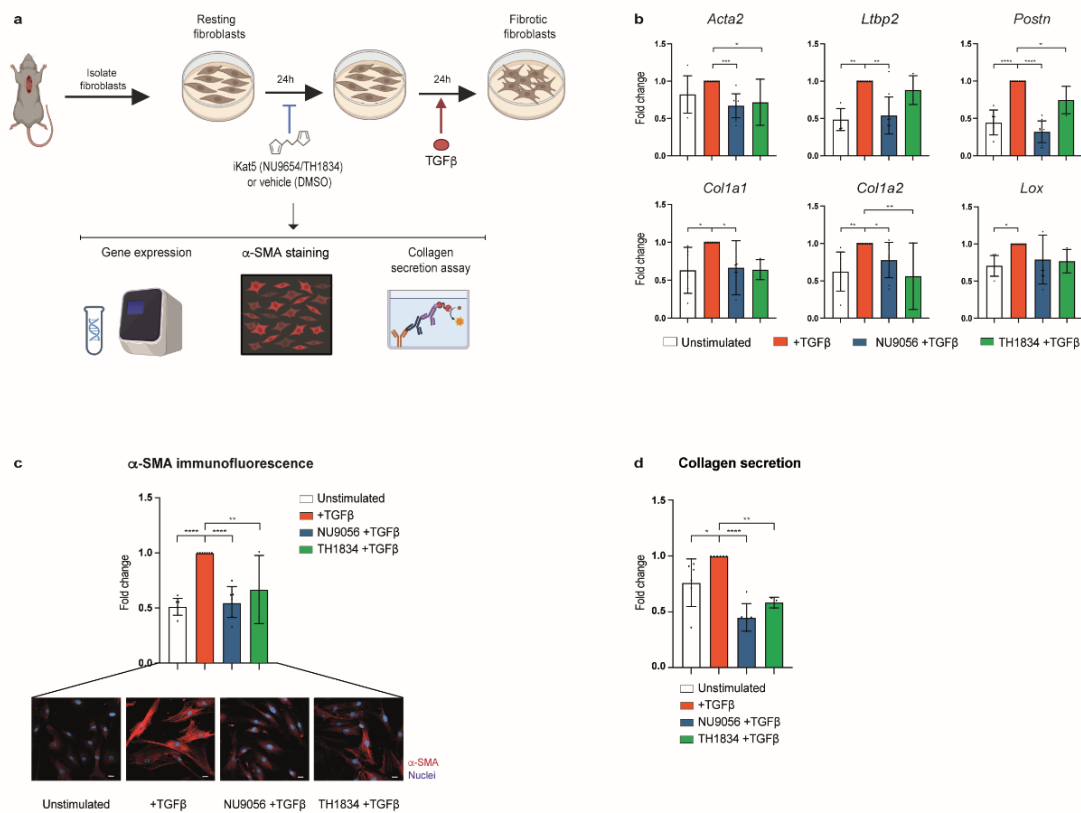


Figure R5Q8 | Kat5 inhibition attenuates fibrotic responses in murine cardiac fibroblasts. (a) Schematic depiction of the experimental approach in murine cardiac fibroblasts. (b) Expression of fibrotic marker genes following TGF- β stimulation in control, NU-9056 and TH1834 pre-treated murine cardiac fibroblasts. The measurements were performed in three-eleven independent experiments. (c) Quantification of the average immunofluorescence intensity of α -SMA, following TGF- β stimulation in control, NU-9056 and TH1834 pre-treated murine cardiac fibroblasts. The measurements were performed in three-seven independent experiments. Representative images of α -SMA immunostaining assays are shown at the bottom. Scale bars: 20 μ m. (d) Quantification of collagen secretion following TGF- β stimulation in control, NU-9056 and TH1834 pre-treated murine cardiac fibroblasts. The measurements were performed in three-six independent experiments. All data are shown as fold change vs. TGF- β values and are mean \pm SD. Statistical significance was analyzed by one-way ANOVA or Kruskal-Wallis tests and is indicated as follows: *P < 0.05, **P < 0.01, ***P < 0.001, ****P < 0.0001.

9. In general, current guidelines suggest that data should not be presented as fold change for experiments other than gene expression. The authors should consider presenting actual data points rather than normalized where feasible.

We acknowledge the general preference to avoid fold change representation in non-transcriptional assays when absolute values are directly comparable. However, we opted for fold change normalization in certain datasets to account for inter-experimental variability and technical differences inherent to fluorescence- or absorbance-based assays. This approach enhances consistency and interpretability across independent experiments. All data are presented with individual data points and appropriate statistical analyses to ensure transparency and reproducibility.

10. The authors should not use the term fibrosis for any of the *in vitro* results. They are simply looking at different fibroblast state. Not fibrosis.

The manuscript has been revised to replace the term “fibrosis” with “fibroblast activation” or “fibrotic transformation,” as appropriate, in the context of *in vitro* findings.

11. The authors should consider listing potential limitations of their conclusions and experiments.

We thank the reviewer for this constructive comment. We have addressed key limitations regarding the elucidation of Kat5’s role in cardiac fibrosis throughout the Discussion, including: (1) the limitations of our *in vitro* system in replicating the heart’s complex 3D environment, (lines 387–391); (2) the potential influence of fibroblast heterogeneity on responses to Kat5 inhibition (lines 401–404); and (3) the limited number of human donors, which constrains the generalizability of our findings and underscores the need for future studies using advanced models and larger cohorts (lines 380–385).

References:

1. Paz-Artigas, L. *et al.* Generation of Self-Induced Myocardial Ischemia in Large-Sized Cardiac Spheroids without Alteration of Environmental Conditions Recreates Fibrotic Remodeling and Tissue Stiffening Revealed by Constriction Assays. *ACS Biomater Sci Eng* **10**, 987–997 (2024).
2. Aghagolzadeh, P. *et al.* Assessment of the Cardiac Noncoding Transcriptome by Single-Cell RNA Sequencing Identifies *FIXER*, a Conserved Profibrogenic Long Noncoding RNA. *Circulation* **148**, 778–797 (2023).
3. Chaffin, M. *et al.* Single-nucleus profiling of human dilated and hypertrophic cardiomyopathy. *Nature* **608**, 174–180 (2022).
4. Turner, R. J. *et al.* A Whole Genome-Wide Arrayed CRISPR Screen in Primary Organ Fibroblasts to Identify Regulators of Kidney Fibrosis. *SLAS Discovery* **25**, 591–604 (2020).